[27] Kouro T, Nagata K, Takaki S, Nisitani S, Hirano M, Wahl MI, et al. Bruton's tyrosine kinase is required for signaling the CD79b-mediated pro-B to pre-B cell transition. Int Immunol 2001;13:485–93.
[28] Sato S, Katagiri T, Takaki S, Kikuchi Y, Hitoshi Y, Yonehara S, et al. IL-5 receptor-mediated tyrosine phosphorylation of SH2/SH3-containing proteins and activation of Bruton's tyrosine and Janus 2 kinases. J Exp Med 1994;180:2101–11.
[29] Matsuda T, Takahashi-Tezuka M, Fukada T, Okuyama Y, Fujitani Y, Tsukada S, et al. Association and activation of Btk and Tec tyrosine kinases by gp130, a signal transducer of the interleukin-6 family of cytokines. Blood 1995;85:627–33.
[30] Sims JE, Williams DE, Morrissey PJ, Garka K, Foxworthe D, Price V, et al. Molecular cloning and biological characterization of a novel murine lymphoid growth factor. J Exp Med 2000;192:671–80.
[31] Liu YJ, Soumelis V, Watanabe N, Ito T, Wang YH, Malefyt Rde W, et al. TSLP: an epithelial cell cytokine that regulates T cell differentiation by conditioning dendritic cell maturation. Annu Rev Immunol 2007;25:193–219.
[32] Park LS, Martin U, Garka K, Gliniak B, Di Santo JP, Muller W, et al. Cloning of the murine thymic stromal lymphopoietin (TSLP) receptor: Formation of a functional heteromeric complex requires interleukin 7 receptor. J Exp Med 2000;192:659–70.
[33] Maki K, Sunaga S, Komagata Y, Kodaira Y, Mabuchi A, Karasuyama H, et al. Interleukin 7 receptor-deficient mice lack γδ T cells. Proc Natl Acad Sci U S A 1996;93:7172–7.
[34] von Freeden-Jeffry U, Vieira P, Lucian LA, McNeil T, Burdach SE, Murray R. Lymphopenia in interleukin (IL)-7 gene-deleted mice identifies IL-7 as a nonredundant cytokine. J Exp Med 1995;181:1519–26.
[35] Levin SD, Koelling RM, Friend SL, Isaksen DE, Ziegler SF, Perlmutter RM, Farr AG. Thymic stromal lymphopoietin: a cytokine that promotes the development of IgM+ B cells in vitro and signals via a novel mechanism. J Immunol 1999;162:677–83.
[36] Isaksen DE, Baumann H, Trobridge PA, Farr AG, Levin SD, Ziegler SF. Requirement for stat5 in thymic stromal lymphopoietin-mediated signal transduction. J Immunol 1999;163:5971–7.
[37] Suzuki H, Terauchi Y, Fujiwara M, Aizawa S, Yazaki Y, Kadowaki T, Koyasu S. Xid-like immunodeficiency in mice with disruption of the p85α subunit of phosphoinositide 3-kinase. Science 1999;283:390–2.
[38] Engel P, Zhou LJ, Ord DC, Sato S, Koller B, Tedder TF, Abnormal. B lymphocyte development, activation, and differentiation in mice that lack or overexpress the CD19 signal transduction molecule. Immunity 1995;3:39–50.
[39] Xu S, Tan JE, Wong EP, Manickam A, Ponniah S, Lam KP. B cell development and activation defects resulting in xid-like immunodeficiency in BLNK/SLP-65-deficient mice. Int Immunol 2000;12:397–404.
[40] Hitoshi Y, Sonoda E, Kikuchi Y, Yonehara S, Nakauchi H, Takatsu K. IL-5 receptor positive B cells, but not eosinophils, are functionally and numerically influenced in mice carrying the X-linked immune defect. Int Immunol 1993;5:1183–90.
[41] Jensen CT, Kharazi S, Boiers C, Cheng M, Lubking A, Sitnicka E, Jacobsen SE. FLT3 ligand and not TSLP is the key regulator of IL-7-independent B-1 and B-2 B Lymphopoiesis. Blood 2008;112:2297–304.
[42] Sitnicka E, Brakebusch C, Martensson IL, Svensson M, Agace WW, Sigvardsson M, et al. Complementary signaling through flt3 and interleukin-7 receptor α is indispensable for fetal and adult B cell genesis. J Exp Med 2003;198:1495–506.
[43] Nagata K, Nakamura T, Kitamura F, Kuramochi S, Taki S, Campbell KS, Karasuyama H. The Igα/Igβ heterodimer on μ-negative proB cells is competent for transducing signals to induce early B cell differentiation. Immunity 1997;7:559–70.
[44] Lang P, Stolpa JC, Freiberg BA, Crawford F, Kappler J, Kupfer A, Cambier JC. TCR-induced transmembrane signaling by peptide/MHC class II via associated Ig-α/β dimers. Science 2001;291:1537–40.
[45] Iwasaki H, Mizuno S, Mayfield R, Shigematsu H, Arinobu Y, Seed B, et al. Identification of eosinophil lineage-committed progenitors in the murine bone marrow. J Exp Med 2005;201:1891–7.
[46] Esplin BL, Welner RS, Zhang Q, Borghesi LA, Kincade PW. A differentiation pathway for B1 cells in adult bone marrow. Proc Natl Acad Sci U S A 2009;106:5773–8.

IL-4/IL-13 antagonist DNA vaccination successfully suppresses Th2 type chronic dermatitis

T. Morioka, K. Yamanaka, H. Mori, Y. Omoto, K. Tokime, M. Kakeda, I. Kurokawa, E.C. Gabazza,* A. Tsubura,† Y. Yasutomi‡ and H. Mizutani

Department of Dermatology and *Department of Immunology, Mie University, Graduate School of Medicine, 2-174 Edobashi, Tsu, Mie 514-8507, Japan
†Department of Pathology II, Kansai Medical University, Moriguchi, Osaka 570-8507, Japan
‡Laboratory of Immunoregulation and Vaccine Research, Tsukuba Primate Research Center, National Institute of Biomedical Innovation, Tsukuba, Ibaraki 305-0843, Japan

Correspondence
Hitoshi Mizutani.
E-mail: h-mizuta@clin.medic.mie-u.ac.jp

Accepted for publication
17 November 2008

Key words
atopic dermatitis, contact hypersensitivity, DNA vaccine, IL-4 mutant

Conflicts of interest
None declared.

DOI 10.1111/j.1365-2133.2009.09069.x

Summary

Background Atopic dermatitis (AD) is a chronic disease with a Th2-type-cytokine dominant profile. Several cytokines and related peptides have been used for the treatment of AD but they were ineffective because of their limited biological half-life. We have recently developed a highly efficient mouse dominant negative interleukin (IL)-4/IL-13 antagonist (IL-4DM), which blocks both IL-4 and IL-13 signal transductions.

Objective To examine the effects of IL-4DM *in vivo* in an AD model induced by the repeated exhibition of oxazolone (OX).

Methods Plasmid DNA was injected intraperitoneally to cause an experimental AD-like dermatitis. The effect was evaluated by ear thickness, histological findings, and mast cells counts in the inflamed skin. The plasma IgE and histamine levels were measured. Cytokine production in skin and splenocytes were also analysed.

Results Mice treated with control plasmid developed marked dermatitis with mast cells and eosinophil infiltration, and had increased plasma IgE and histamine levels with a Th2 type splenocyte cytokine profile. Treatment with mouse IL-4 DNA augmented the ear swelling and thickness with an increased dermal eosinophil count, plasma histamine level, and production of splenocyte IL-4. However, IL-4DM treatment successfully controlled the dermatitis, decreased the mast cell and eosinophil count, and suppressed plasma IgE and histamine levels. Splenocytes produced an increased level of IFN-γ.

Conclusion These data showed that the simultaneous suppression of IL-4/IL-13 signals successfully controlled Th2-type chronic dermatitis. IL-4DM DNA treatment is a potent therapy for AD and related diseases.

Interleukin (IL)-4 plays a central role in Th2-cytokine-dominant inflammatory skin diseases such as atopic dermatitis (AD).[1–3] IL-4 is responsible for the differentiation of allergen-specific Th2 cells together with its closely related cytokine IL-13 for the class switching of activated B cells to IgE-producing cells. The effects of IL-13 are similar to IL-4 on B cells, monocytes, and other cell types, but T cells appear to lack an IL-13 binding receptor component and do not respond to IL-13.[4] The structural basis for the overlapping functions of IL-4 and IL-13 is a shared receptor subunit, and IL-4Rα organizes intracellular signals in response to both cytokines.[5,6] Signal transduction is induced by heterodimerization of the IL-4Rα with a second subunit; which may vary according to the cell types. The specific inhibition of IL-4 can be achieved by antagonistic IL-4 mutants. Variants of human IL-4 that bind to the receptor subunit IL-4Rα, but not to the other subunit γ-chain (γc) or IL-13Rα1 are competitive antagonists of IL-4.[7,8] IL-13 is inhibited by similar variants, which form unproductive complexes with IL-4Rα.[5,9] The single-site human IL-4 mutant Y124D has been used as an IL-4/IL-13 inhibitor in various studies,[7–17] but this variant retains some residual agonistic activity, which could be relevant for *in vivo* applications.[7,8] In contrast, IL-4 and IL-13 double mutant R121D/Y124D lacks detectable activity and appears to be an effective antagonist for human IL-4 and IL-13.[5,18]

We have recently developed a highly efficient murine IL-4 antagonist DNA (IL-4DM), in which the amino acids glutamine 116 and tyrosine 119 were changed for aspartic acid.[19] This murine mutant DNA is analogous to the R121D/Y124D double mutant. IL-4DM binds with high affinity to the murine

IL-4Rα without inducing signal transduction, and has no detectable activity upon the proliferation or differentiation of murine cells. An appropriate amount of IL-4DM completely inhibits responses by wild-type IL-4.[19] Like its human analogue, the IL-4DM mutant is also an antagonist of IL-13 (B. Schnarr *et al.*, unpublished data[37]). Recent experiments with monocytes from mice lacking a functional γc gene showed that IL-4DM is a complete inhibitor of IL-4 in the absence of γc as well.[20] In this study we have examined the effects of IL-4DM *in vivo*, using an AD model induced by the repeated exhibition of oxazolone (OX). The repeated application of a hapten such as OX on mice causes an initial delayed-type hypersensitivity that changes to an immediate-type response in the late phase with elevated IgE production and deviation of Th-cell responses. The skin lesions that appear in the late phase are compatible with the clinical findings as well as the cytokine profile observed in AD.[21–23] The inhibitory effect of IL-4DM on IL-4 and IL-13 on the immune response was comparable with that of knockout mice lacking either IL-4[24] or IL-4Rα. Treatment with IL-4DM prevented contact hypersensitivity responses with the increased production of interferon (IFN)-γ.

Materials and methods

Animals

BALB/c male mice aged 5 weeks were purchased from Japan SLC Co. (Shizuoka, Japan) and were used at the age of 6 weeks. Age-matched wild-type BALB/c mice were used as controls. All animals were cared for according to the ethical guidelines approved by the Institutional Animal Care and Use Committee of Mie University.

Reagents

The cDNA coding region of mouse IL-4 was amplified by a polymerase chain reaction (PCR) based on the cDNA sequence of mouse IL-4. The mouse IL-4 fragment was inserted into BamHI and EcoRI-filled in pcDNA3.1+ (Invitrogen, San Diego, CA, U.S.A.) under the TPA leader sequence, and then digested by BamHI and SacI. A Quickchange™ Site-directed Mutagenesis kit (Stratagene, La Jolla, CA, U.S.A.) was used for the mutagenesis of mouse IL-4. The oligonucleotide primers used to prepare a mouse IL-4 double mutant (IL-4DM, Q116D/Y119D) were CTAAAGAGCATCATGGATATGGATGACTCGTAGTCTAGAG and CTCTAGACTACGAGTCATCCATATCCATGATGCTCTTTAG. The IL-4 mutant fragments were ligated into pcDNA3.1+.[25] Mouse IL-4, IL-4DM plasmid DNAs were purified using the Plasmid Mega kit (Qiagen, Chatsworth, CA, U.S.A.) and diluted with sterilized physiological saline. OX was purchased from Sigma (St Louis, MO, U.S.A.) and was dissolved in acetone/olive oil (4 : 1).

Administration of DNA

Mice were treated by intraperitoneal injection of 100 μg of IL-4DM DNA on days 0, 7, 14, 21 and 28. A control plasmid (pcDNA3.1+) vector and IL-4 DNA were also injected on the same day (Fig. 1).

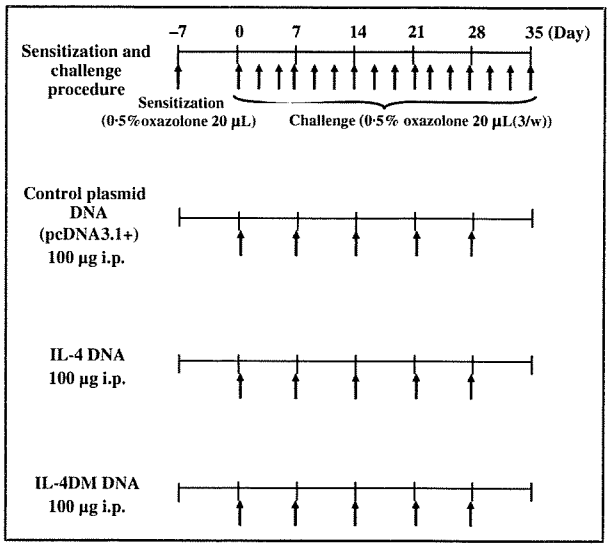

Fig 1. Schedule for induction of chronic contact hypersensitivity and administration of compounds. Mice received intraperitoneal (i.p.) injection of 100 μg of each plasmid DNA on days 0, 7, 14, 21 and 28.

Sensitization and challenge procedures

As shown in Figure 1, mice were initially sensitized by pasting 20 μL of 0·5% OX solution to their left ear 7 days before the first challenge (day 7) and then 20 μL of 0·5% OX solution was repeatedly applied on the left ear three times per week from day 0 as reported previously.[23] Ear swelling was measured with thickness gauge calipers before and 30 min after OX challenge to the pinna of the ear on day 35. The ear swelling response was expressed as the difference between the values taken before and 30 min after application.

Histological analysis

Ear skin specimens obtained 6 h after the final challenge on day 35 were fixed in 10% buffered neutral formaldehyde and embedded in paraffin wax. Histological sections were of 6 μm thickness and they were stained with haematoxylin and eosin. The sections were also stained with 0·5% toluidine blue for the identification of mast cells. The cell counts were performed in six consecutive microscopic fields at × 400 magnification.

Measurement of plasma IgE and plasma histamine

Blood was collected under ether anaesthesia 6 h after the last challenge. Plasma IgE levels were determined by a sandwich enzyme-linked immunosorbent assay (ELISA). In brief, 96-well immunoplates (Corning Inc., Corning, NY, U.S.A.) were coated with 100 μL of an antimouse IgE capture antibody (2 μg mL^{-1}) (BD PharMingen, San Diego, CA, U.S.A.) overnight at 4 °C. Plasma samples of 100 μL were diluted 60-fold with PBS

containing 10% fetal calf serum (FCS) were placed in the wells. After incubation for 1 h at room temperature, 100 μL of biotin-conjugated antimouse IgE antibody (2 μg mL^{-1} in blocking buffer) (BD PharMingen) was added to each well. The plates were incubated at room temperature for 1 h, followed by six washes, incubated with 100 μL of horseradish peroxidase avidin D (FUNAKOSHI, Tokyo, Japan) 1 : 1000 in blocking buffer, and then incubated for 30 min at room temperature. A substrate solution of 100 μL containing 1·5 mg ABTS (Sigma-Aldrich, St Louis, MO, U.S.A.) in 5 mL of a 0·1 mol L^{-1} citric acid solution was added, and kept for 30 min at room temperature in a dark place. Thereafter the reaction was terminated by adding 50 μL of 2 mol L^{-1} H_2SO_4, and the optical density of each well at 405 nm was determined by using a microplate reader. A standard curve was prepared using mouse anti-TNP IgE standard (BD PharMingen). Plasma histamine levels were analysed using the commercial sandwich ELISA kit from Immunoteck (Marseille, France) according to the manufacturer's protocol.

Purification of mRNA from mouse ears

At 6 h after the final challenge, the skin of the left ear was sampled. The specimen was homogenized and the total RNA was extracted using Isogen (Nippon Gene, Tokyo, Japan) according to the manufacturer's instruction; 1 mL of homogenate was vigorously mixed with 200 μL of chloroform, and centrifuged at 12 000 g for 15 min at 4 °C. The aqueous phase was separated and mixed with 0·5 mL of 2-propanol (Nacalai Tesque, Kyoto, Japan) to precipitate RNA. After centrifugation, the precipitate was washed with 1 mL of 75% ethanol (Nacalai Tesque) and dried. RNA was suspended in 50 μL of RNase-free water, and the concentration was measured based on the absorbance at 260 nm, and the quality was confirmed by electrophoresis. cDNA was prepared from 10 μg of mRNA using archive kit (ABI, Foster City, CA, U.S.A.) according to the manufacturer's protocol.

Cytokine mRNA expression in skin

The transcriptional activity in the lesional skin samples was measured with a PCR. The amplification of cDNA was performed in 50 μL of a master mixture containing 0·5 μg of cDNA, 200 nmol deoxynucleotide triphosphate, 5 μL of PCR buffer, 2 U of Taq polymerase (ABI) and 2 μmol of each specific primer for the DNA of interest. The following primers were used for PCR reactions (5′–3′), mouse IFN-γ: TCAAGTGGCATAGATGTGGAAGAA and TGGCTCTGCAGGATTTTCATG; mouse IL-2: CCTGAGCAGGATGGAGAATAACA and TCCAGAACATGCCGCAGAG; mouse IL-4: CACTGACGGCACAGAGCTATTGATG and TCATGGTGCAGCTTTCGATGAATC; mouse IL-10: CTCTTACTGACTGGCATGAGGATCAGCAGG and TCTTCACCTGCTCCACTGCCTTGCTCTTAT; mouse IL-12: TCCTGCACTGCTGAAGACATC and TCTCGCCATTATAGATTCAGAGAC; mouse IL-13: AGACCAGACTCCCCTGTGCA and TGGGTCCTGTAGATGGCATTG; mouse β-actin: TGGAATCCTGTGGCATCCATGAAAC and TAAAACGCAGCTCAGTAACAGTCCG.[26] PCR was performed under the following conditions: 95 °C for 5 min, followed by 35 or 40 cycles of 95 °C for 30 s, 56 °C (IFN-γ, IL-12) or 60 °C (IL-2, IL-4, IL-10, IL-13, β-actin) for 30 s, and 72 °C for 1 min were carried out. After the final cycle, the temperature was maintained at 72 °C for 7 min. PCR amplified fragments were electrophoresed through 1·5% agarose gels in tris-acetate EDTA buffer containing ethidium bromide, and the gels were scanned under ultraviolet light. The mRNA of β-actin was used as an internal control. The signal intensity of each reverse transcriptase (RT)-PCR product was estimated using an ATTO Lane & Spot Analyzer (ATTO, Shizuoka, Japan).

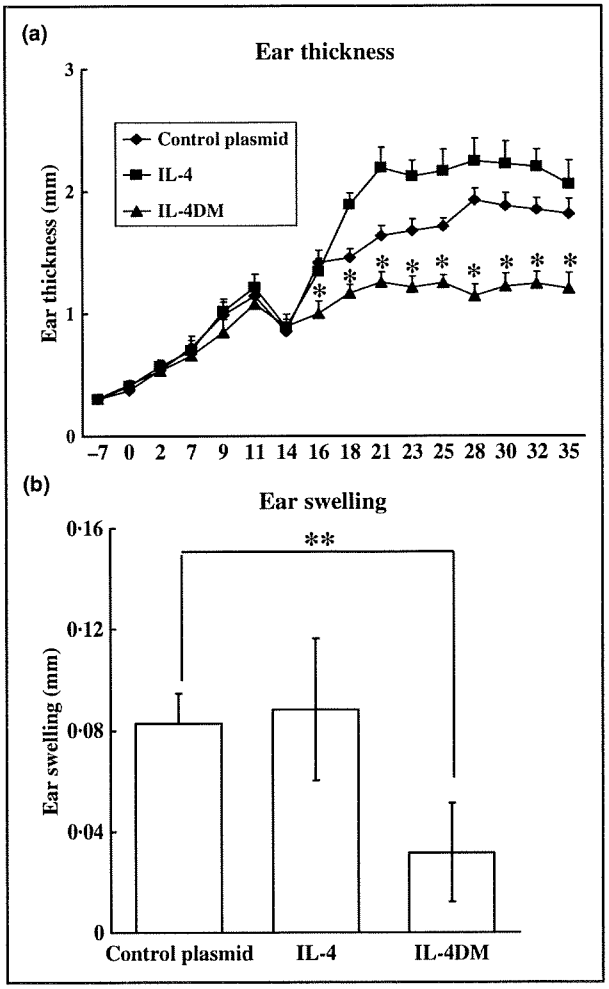

Fig 2. The effects of interleukin (IL)-4DM, IL-4, and control plasmid (pcDNA3.1) on ear swelling induced by repeated application of oxazolone (OX). (a) Ear thickness was measured before each OX challenge. Each point represents the mean ± SD of seven or eight mice. *$P < 0·05$: significantly different from the control group and IL-4 (Student's t-test). (b) Inhibition of the effecter phase of chronic hypersensitivity by IL-4DM, IL-4, and control plasmid DNA transfer. The ear swelling was measured 30 min after applying OX. The ear swelling in the IL-4DM groups was significantly suppressed compared with those in the IL-4 and control plasmid DNA groups. *Significant difference from the control by Student's t-test at $P < 0·05$.

Cytokine production from splenocytes

A suspension of 2×10^6 splenocytes were made in a solution of 200 μL RPMI-1640 medium (Nikken Bio Medical Laboratory, Kyoto, Japan) containing 10% fetal bovine serum (FBS; Biowest, Nuaillé, France), 50 UI penicillin, 50 μg mL^{-1} streptomycin, and 5 μg mL^{-1} soluble antimouse CD3 (BD Bioscience), and 10 μg mL^{-1} antimouse CD28 (BD Bioscience). Cells were dispensed in triplicate into 96-well flat-bottomed microplates (Sumitomo Bakelite, Tokyo, Japan). After incubation for 48 h at 37 °C in a humidified incubator (5% CO_2), culture supernatants were collected and analysed for IFN-γ (Quantikine; R&D Systems, Minneapolis, MN, U.S.A.) or IL-4 (Quantikine; R&D Systems) production with an ELISA according to the manufacturer's protocol.

Statistical analysis

Statistical analysis was performed using Student's t-test and Mann–Whitney U-test. Values are expressed as mean ± SEM. A 95% confidence limit was taken as significant ($P < 0.05$).

Result

Ear thickness with the treatment of IL-4DM, IL-4, or control plasmid

In the control group, the ear thickness increased from the beginning of the challenge, and increased gradually through the experiments (Fig. 2a). The agonistic IL-4 DNA treatment augmented increase of the ear thickness after day 16. In contrast, IL-4DM DNA treatment significantly suppressed increase of the ear thickness compared with that of control plasmid or IL-4DNA-treated mice.

Effects of IL-4DM on the oxazolone-induced acute-phase ear swelling

The ear swelling was also measured 30 min after OX application on day 35, and the difference between before and 30 min after application was calculated. IL-4DM DNA treatment suppressed the ear swelling significantly compared with that of the control DNA-injected group (Fig. 2b). However, IL-4DNA showed no suppressive effects.

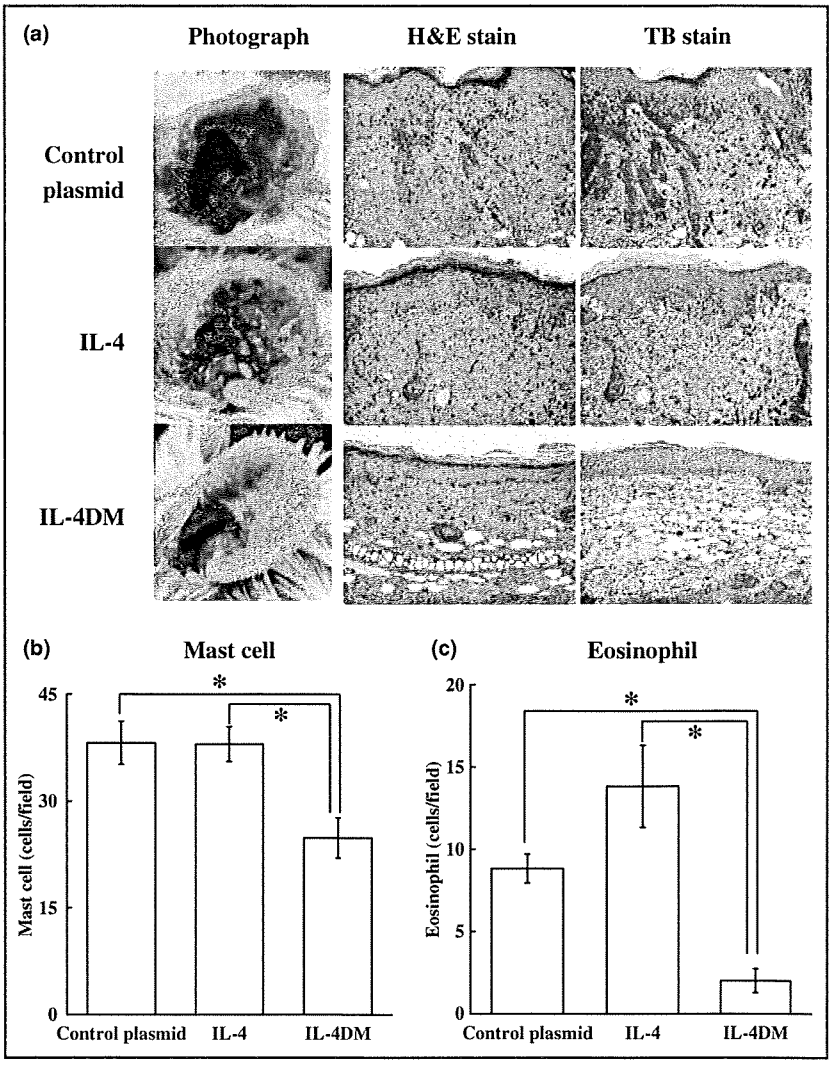

Fig 3. (a) Representative photographs and histological feature of oxazolone (OX)-treated skin lesion. OX-sensitized ear revealed hyperkeratosis, acanthosis, and parakeratosis in control and interleukin (IL)-4-treated mice. An increased number of infiltrating lymphocytes, macrophages and mast cells was observed in the skin lesions, all of which are typical histological findings observed in patients with atopic dermatitis. In contrast, acanthosis was clearly suppressed, and skin infiltration of granulocytes, eosinophils, and mast cells was decreased in the IL-4DM-treated mice as compared with control plasmid-treated mice (original magnification × 200). (b) The number of dermal mast cells was counted, and found to be decreased in the IL-4DM-treated mice. (c) The number of dermal eosinophils was also counted in 10 high power fields. The skin infiltration of eosinophils was significantly decreased in the IL-4DM-treated mice. Data are expressed as the mean ± SEM. *Significant difference by Student's t-test at $P < 0.05$.

Histological findings and mast cell counts in the inflamed skin

In control plasmid-treated mice and IL-4 DNA-treated mice, severe dermatitis was observed on the earlobe. A drastic decrease of inflammation was observed in IL-4DM DNA-treated mice (Fig. 3a). Histological examination on the OX-challenged ear skin revealed hyperkeratosis, acanthosis and parakeratosis in both of the control and IL-4-treated mice. An increased number of infiltrating lymphocytes, macrophages and mast cells was observed in the skin lesions in control DNA and IL-4 DNA-treated mice. These findings are comparable with those of AD skin lesions. In contrast, the acanthotic changes and infiltration of granulocytes, mast cells, and eosinophils were significantly suppressed in the IL-4DM DNA-treated mice compared with those of control DNA- or IL-4 DNA-treated mice (Fig. 3b,c). Interestingly, IL-4 DNA treatment increased eosinophil counts compared with control DNA treatment.

Plasma IgE and histamine levels

The total plasma IgE level was increased by repeated OX challenges (Fig. 4a). IL-4 DNA treatment showed no agonistic effects in the plasma IgE level; however, IL-4DM DNA treatment significantly suppressed the levels of plasma IgE. The plasma histamine level was also significantly increased in the control DNA- or IL-4 DNA-treated mice; however, IL-4DM DNA treatment significantly suppressed the plasma histamine levels (Fig. 4b).

Cytokine mRNA expression levels

To determine the effects of IL-4DM on cytokine production in the inflamed skin lesions, mRNA expression of Th1 and Th2 cytokines was analysed. The IFN-γ mRNA expression was significantly increased in IL-4DM DNA-treated mice ear compared with that of control DNA-treated samples (standardized by β-actin expression).

However, no remarkable difference in other cytokine mRNA expression was observed among three different DNA-treated samples (Fig. 5a,b).

Concentration of IFN-γ and IL-4 in splenocyte cell culture supernatants

To know the effects of IL-4DM DNA therapy in the systemic immune system, the concentration of IFN-γ in splenocyte cell culture supernatants was measured by ELISA. The IFN-γ level in the IL-4DM-treated samples was significantly higher than that in the control DNA- or IL-4 DNA-treated samples (Fig. 6a). We also measured the concentration of IL-4 in splenocyte cell culture supernatants by ELISA for mouse IL-4. The IL-4 level in the IL-4DM-treated samples was as high as the IL-4 DNA-treated samples. These were higher than that of the control DNA-treated samples (Fig. 6b).

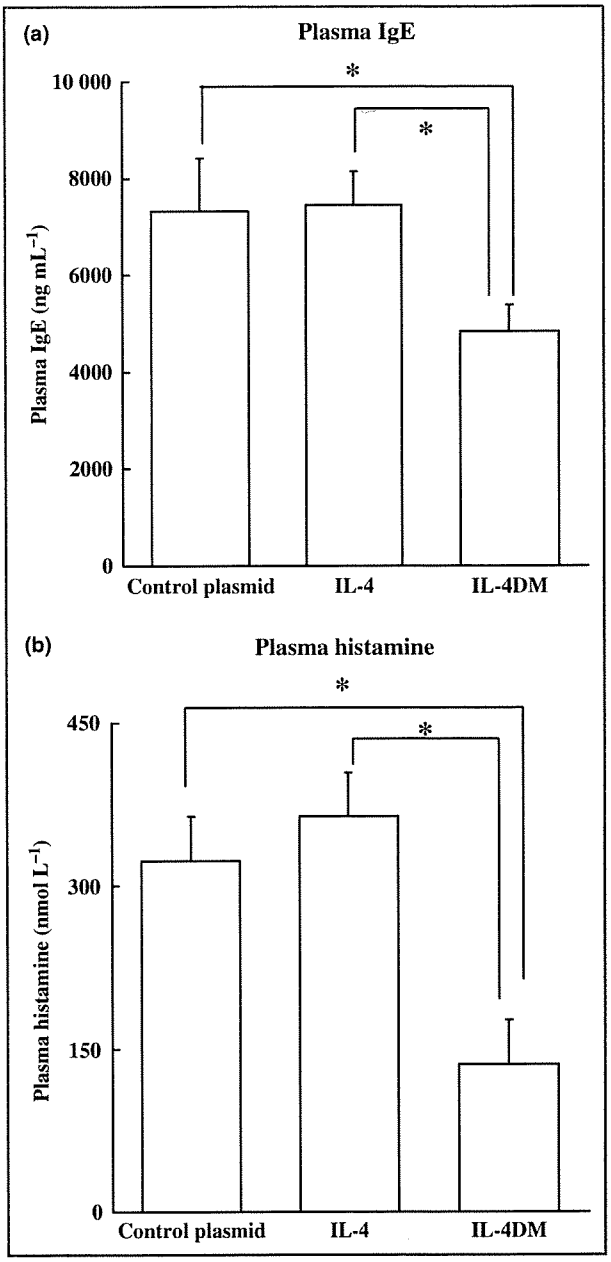

Fig 4. Plasma IgE and histamine levels. (a) Plasma IgE level was decreased in interleukin (IL)-4DM treated mice. (b) Inhibition of the production of plasma histamine was observed in IL-4DM DNA-treated mice. *Significant difference from the IL-4 and control by Mann–Whitney U-test at $P < 0{\cdot}05$.

Discussion

Several previous studies have shown that AD is a chronic dermatitis with a predominance of Th2 cytokines in the lesional skin,[27–29] and that Th2 cytokines play a critical role in the pathogenesis of dermatitis.[28] IL-4 is one of the Th2 cytokines that affects the function of different cell types including T cells, B cells, mast cells, monocytes/macrophages, endothelial cells, fibroblasts, dendritic cells, Langerhans cells

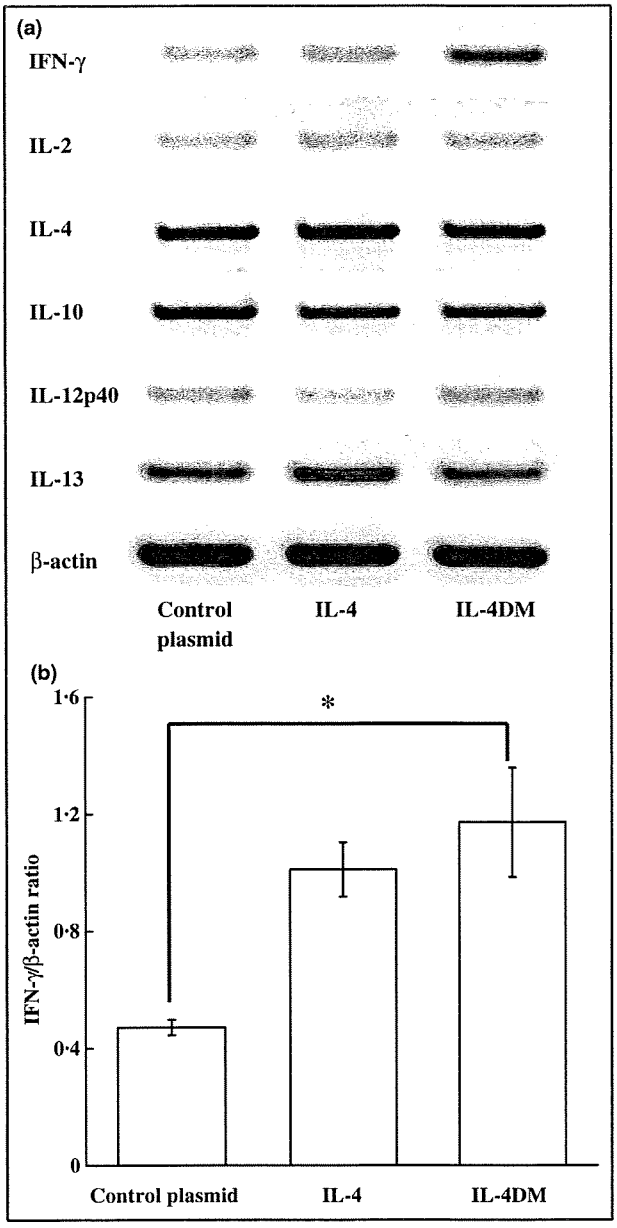

Fig 5. (a) Reverse-transcriptase polymerase chain reaction analysis of cytokine mRNA expression 6 h after oxazolone (OX)-sensitization. The cDNAs were amplified for respective cycles of six cytokines and β-actin, subjected to electrophoresis, and visualized with ethidium bromide. Representative results under optimal conditions are shown. Although almost all Th1 and Th2 cytokine levels were unchanged, mRNA expression for interferon (IFN)-γ was increased in IL-4DM-treated mice. (b) The level of mRNA expression of IFN-γ was expressed as the value relative to that for β-actin. The IFN-γ level in the IL-4DM group is significantly higher than that of control plasmid groups. *Significant difference from the control by Student's t-test at $P < 0{\cdot}05$.

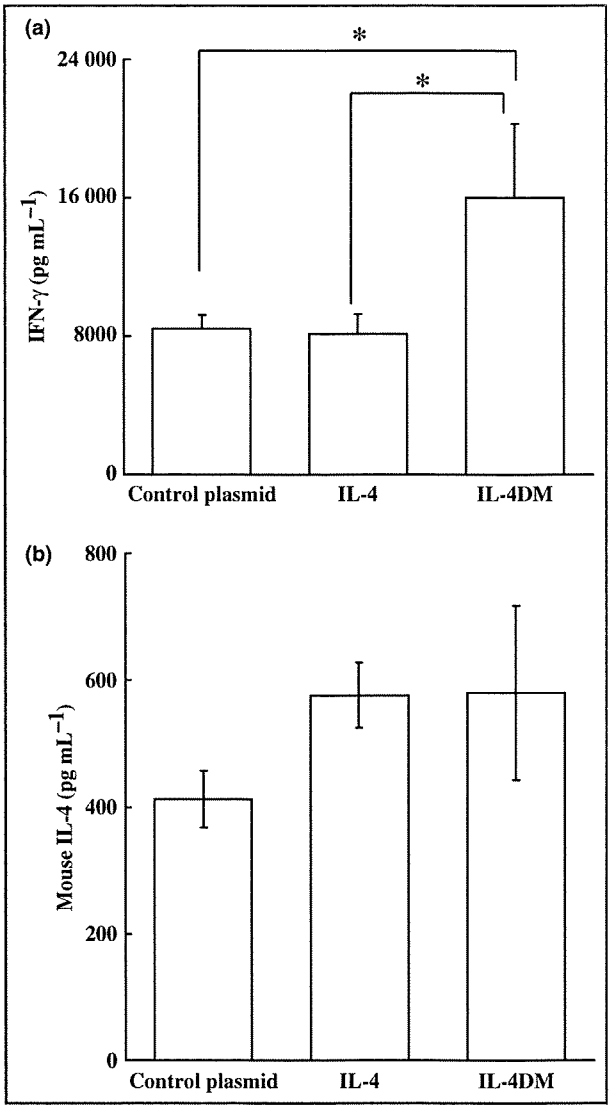

Fig 6. Cytokine production from splenocytes in chronic hypersensitivity mice. Interferon (IFN)-γ and interleukin (IL)-4 production from splenocytes was measured. (a) Actual IFN-γ protein production was increased in the IL-4DM-treated mice. (b) IL-4 levels did not reach the significance, but showed a tendency to increase in the IL-4 and IL-4DM mice. *Significant difference from the control by Mann–Whitney U-test at $P < 0{\cdot}05$.

and keratinocytes. Because of this broad-spectrum action, IL-4 is believed to play a crucial role in the pathogenesis of AD.[30,31] In the present study, we employed a contact hypersensitivity model by the repeated application of OX, which mimics the histological phenotype of AD in humans; this model also showed increased levels of Th2 cytokines in the lesional skin as reported by Kitagaki *et al.*[21]

Immunotherapy such as the direct blocking of Th2 responses with neutralizing antibody against Th2 cytokines, the soluble form of IL-4 receptor (IL-4R), or antagonistic IL-4 mutant proteins have been used for the treatment of asthma.[32–34] These proteins directly inhibit IL-4 binding thereby inhibiting host immune responses. A previous study by Nishikubo *et al.*[25] showed inhibition of immune responses by using IL-4 mutant protein for at least 50 weeks. However, results from these experimental animals have shown that the application of these trials to humans is difficult. Because the pharmacokinetic half-life of IL-4 mutant and sIL-4R protein

are very short *in vivo* (IL-4 mutant: $t_{1/2}$ = 0·83 h; sIL-4R: $t_{1/2}$ = 4·6 h),[35,36] huge amounts of these molecules are required in plasma to maintain a long period of inhibitory action on allergic inflammation. In fact, administration of these molecules was required many times in high doses from the sensitization to the challenge periods.[35–37] In the present study, we demonstrated a remarkable antagonistic effect of IL-4 mutant DNA applied in a form of vaccination, as a potent new type of immunogene therapy for AD. In previous studies in which gene therapy and DNA vaccines were used in combination with a cytokine gene for tumours or pathogens, effective immune responses to antigen were recognized even in the absence of detectable plasma levels of cytokines. Recently, we also reported that administration of plasmid DNA coding IL-4 cDNA completely inhibited the development of insulitis, which is one of the Th1-type autoimmune diseases, although no IL-4 was detected in plasma.[38] These results suggest that genes applied as a DNA vaccine express and supply products to the host continuously. To occupy the IL-4/IL-13 receptors, a continuous supply of IL-4DM is needed but not bolus application. Therefore, IL-4DM applied as a DNA vaccine might inhibit the allergic inflammation by persistent secretion of mutant IL-4 over a long period in a limited amount.

As we had expected, IL-4DM mitigated phenotypical and histological changes such as severe oedema, inflammatory cell infiltration and epidermal hyperplasia. IL-4DM also significantly decreased the number of dermal mast cells. IL-4 is known to be a potent activator of mast cells. Mast cells, which participate in the inflammatory cascade, serve as an abundant source of Th2 cytokines as well as inflammatory mediators.[39–41] Therefore, inhibition of mast cell activation is another possible mechanism through which IL-4DM ameliorates inflammatory responses in the present model of dermatitis. Eosinophil infiltration into the dermis has been well documented in AD.[42] In this study, an increased number of eosinophils was observed in contact hypersensitivity skin lesions, and was dramatically inhibited by IL-4DM treatment. Inhibition of cellular infiltration in IL-4DM mice may be due to suppression of IL-4-mediated immunological events such as a decreased expression of cellular adhesion molecules on endothelial cells.[43]

Injected IL-4DM and IL-4 DNA are trapped by monocytes/macrophages by phagocytosis. They may migrate to lymph nodes or spleen and show systemic effects. In fact, we could observe a high concentration of IL-4 in cultured splenocytes from IL-4DM DNA injected mice by ELISA. Unfortunately, there is no specific anti-IL-4DM antibody or anti-IL-4DM ELISA. The standard ELISA used in this study could not differentiate the natural mouse IL-4 and mutant IL-4 protein; these findings are consistent with the previous report.[25] The plasma IL-4 levels in the agonistic IL-4DNA-treated mice were consistent with those of the IL-4DM DNA-treated mice. Therefore, we speculate that exogenously applied IL-4DM DNAs were expressed the same as IL-4 DNAs, and showed systemic immunological effects.

IFN-γ production increased systemically and locally in mice treated with IL-4DM DNA. Repeated OX treatments cause expansion both of Th1 and Th2 cells. IL-4DM DNA therapy interfered with the development of the Th2 milieu. Subsequently, IFN-γ production and mRNA expression might become abundant locally and systemically.

Tissue-specific gene transfer could be achieved naturally and effectively through the cell specificity of virus receptors.[44] However, there may be a risk of vector toxicity through viral infection of host cells. Also, the limited size of transgenes is often a serious obstacle. Moreover, immune responses to viral vectors are also induced, and the effects of transgenes are eliminated by immune responses to the vectors. For human applications, the efficacy and safety of any delivery system for gene transfer are always of major concern. Nonviral approaches are advantageous in immunogene therapy. DNA vaccines are capable of inducing potent biological effects in a variety of experimental systems.[45] One of the characteristic features of DNA vaccines is their ability to induce long-lasting immunity. The animals that had been treated with IL-4DM DNA did not develop severe allergic inflammation even before or after antigen sensitization.

In the present study, we showed the beneficial effects of immunogene therapy with IL-4 mutant DNA in an experimental model for AD. An IL-4 mutant DNA vaccination is a potent new tool for the systemic treatment of AD.

Acknowledgments

Grants-in-Aid for Scientific Research and Grants-in-Aid for Core Research Evolutional Science and Technology.

References

1 Paul WE. Interleukin-4: a prototypic immunoregulatory lymphokine. *Blood* 1991; **77**:1859–70.
2 Mosmann TR, Sad S. The expanding universe of T-cell subsets: Th1, Th2 and more. *Immunol Today* 1996; **17**:138–46.
3 Romagnani S. The Th1/Th2 paradigm. *Immunol Today* 1997; **18**:263–6.
4 Zurawski G, de Vries JE. Interleukin 13, an interleukin 4-like cytokine that acts on monocytes and B cells, but not on T cells. *Immunol Today* 1994; **15**:19–26.
5 Tony HP, Shen BJ, Reusch P *et al.* Design of human interleukin-4 antagonists inhibiting interleukin-4-dependent and interleukin-13-dependent responses in T-cells and B-cells with high efficiency. *Eur J Biochem* 1994; **225**:659–65.
6 Smerz-Bertling C, Duschl A. Both interleukin 4 and interleukin 13 induce tyrosine phosphorylation of the 140-kDa subunit of the interleukin 4 receptor. *J Biol Chem* 1995; **270**:966–70.
7 Kruse N, Tony HP, Sebald W. Conversion of human interleukin-4 into a high affinity antagonist by a single amino acid replacement. *EMBO J* 1992; **11**:3237–44.
8 Kruse N, Shen BJ, Arnold S *et al.* Two distinct functional sites of human interleukin 4 are identified by variants impaired in either receptor binding or receptor activation. *EMBO J* 1993; **12**:5121–9.
9 Zurawski SM, Vega F Jr, Huyghe B *et al.* Receptors for interleukin-13 and interleukin-4 are complex and share a novel component that functions in signal transduction. *EMBO J* 1993; **12**:2663–70.

10 Aversa G, Punnonen J, Cocks BG *et al.* An interleukin 4 (IL-4) mutant protein inhibits both IL-4 or IL-13-induced human immunoglobulin G4 (IgG4) and IgE synthesis and B cell proliferation: support for a common component shared by IL-4 and IL-13 receptors. *J Exp Med* 1993; **178**:2213–18.
11 Zurawski SM, Chomarat P, Djossou O *et al.* The primary binding subunit of the human interleukin-4 receptor is also a component of the interleukin-13 receptor. *J Biol Chem* 1995; **270**:13869–78.
12 Konig B, Fischer A, Konig W. Modulation of cell-bound and soluble CD23, spontaneous and ongoing IgE synthesis of human peripheral blood mononuclear cells by soluble IL-4 receptors and the partial antagonistic IL-4 mutant protein IL-4 (Y124D). *Immunology* 1995; **85**:604–10.
13 Carballido JM, Schols D, Namikawa R *et al.* IL-4 induces human B cell maturation and IgE synthesis in SCID-hu mice. Inhibition of ongoing IgE production by *in vivo* treatment with an IL-4/IL-13 receptor antagonist. *J Immunol* 1995; **155**:4162–70.
14 Carballido JM, Aversa G, Schols D *et al.* Inhibition of human IgE synthesis *in vitro* and in SCID-hu mice by an interleukin-4 receptor antagonist. *Int Arch Allergy Immunol* 1995; **107**:304–7.
15 Schnyder B, Lugli S, Feng N *et al.* Interleukin-4 (IL-4) and IL-13 bind to a shared heterodimeric complex on endothelial cells mediating vascular cell adhesion molecule-1 induction in the absence of the common gamma chain. *Blood* 1996; **87**:4286–95.
16 Sornasse T, Larenas PV, Davis KA *et al.* Differentiation and stability of T helper 1 and 2 cells derived from naive human neonatal CD4+ T cells, analyzed at the single-cell level. *J Exp Med* 1996; **184**:473–83.
17 Vannier E, de Waal Malefyt R, Salazar-Montes A *et al.* Interleukin-13 (IL-13) induces IL-1 receptor antagonist gene expression and protein synthesis in peripheral blood mononuclear cells: inhibition by an IL-4 mutant protein. *Blood* 1996; **87**:3307–15.
18 Schnarr B, Ezernieks J, Sebald W *et al.* IL-4 receptor complexes containing or lacking the gamma C chain are inhibited by an overlapping set of antagonistic IL-4 mutant proteins. *Int Immunol* 1997; **9**:861–8.
19 Grunewald SM, Kunzmann S, Schnarr B *et al.* A murine interleukin-4 antagonistic mutant protein completely inhibits interleukin-4-induced cell proliferation, differentiation, and signal transduction. *J Biol Chem* 1997; **272**:1480–3.
20 Andersson A, Grunewald SM, Duschl A *et al.* Mouse macrophage development in the absence of the common gamma chain: defining receptor complexes responsible for IL-4 and IL-13 signaling. *Eur J Immunol* 1997; **27**:1762–8.
21 Kitagaki H, Fujisawa S, Watanabe K *et al.* Immediate-type hypersensitivity response followed by a late reaction is induced by repeated epicutaneous application of contact sensitizing agents in mice. *J Invest Dermatol* 1995; **105**:749–55.
22 Kitagaki H, Kimishima M, Teraki Y *et al.* Distinct *in vivo* and *in vitro* cytokine profiles of draining lymph node cells in acute and chronic phases of contact hypersensitivity: importance of a type 2 cytokine-rich cutaneous milieu for the development of an early-type response in the chronic phase. *J Immunol* 1999; **163**:1265–73.
23 Mori H, Yamanaka K, Matsuo K *et al.* Administration of Ag85B showed therapeutic effects to Th2-type cytokine-mediated acute phase atopic dermatitis by inducing regulatory T cells. *Arch Dermatol Res* 2009; **301**:151–7.
24 Kopf M, Le Gros G, Bachmann M *et al.* Disruption of the murine IL-4 gene blocks Th2 cytokine responses. *Nature* 1993; **362**:245–8.
25 Nishikubo K, Murata Y, Tamaki S *et al.* A single administration of interleukin-4 antagonistic mutant DNA inhibits allergic airway inflammation in a mouse model of asthma. *Gene Ther* 2003; **10**:2119–25.
26 Overbergh L, Valckx D, Waer M *et al.* Quantification of murine cytokine mRNAs using real time quantitative reverse transcriptase PCR. *Cytokine* 1999; **11**:305–12.
27 Kay AB, Ying S, Varney V *et al.* Messenger RNA expression of the cytokine gene cluster, interleukin 3 (IL-3), IL-4, IL-5, and granulocyte/macrophage colony-stimulating factor, in allergen-induced late-phase cutaneous reactions in atopic subjects. *J Exp Med* 1991; **173**:775–8.
28 Herz U, Bunikowski R, Renz H. Role of T cells in atopic dermatitis. New aspects on the dynamics of cytokine production and the contribution of bacterial superantigens. *Int Arch Allergy Immunol* 1998; **115**:179–90.
29 Akdis CA, Akdis M, Trautmann A *et al.* Immune regulation in atopic dermatitis. *Curr Opin Immunol* 2000; **12**:641–6.
30 Ricci M, Matucci A, Rossi O. IL-4 as a key factor influencing the development of allergen-specific Th2-like cells in atopic individuals. *J Investig Allergol Clin Immunol* 1997; **7**:144–50.
31 Elbe-Burger A, Egyed A, Olt S *et al.* Overexpression of IL-4 alters the homeostasis in the skin. *J Invest Dermatol* 2002; **118**:767–78.
32 Zhou CY, Crocker IC, Koenig G *et al.* Anti-interleukin-4 inhibits immunoglobulin E production in a murine model of atopic asthma. *J Asthma* 1997; **34**:195–201.
33 Tomaki M, Zhao LL, Lundahl J *et al.* Eosinophilopoiesis in a murine model of allergic airway eosinophilia: involvement of bone marrow IL-5 and IL-5 receptor alpha. *J Immunol* 2000; **165**:4040–50.
34 Bost KL, Holton RH, Cain TK *et al.* *In vivo* treatment with anti-interleukin-13 antibodies significantly reduces the humoral immune response against an oral immunogen in mice. *Immunology* 1996; **87**:633–41.
35 Henderson WR Jr, Chi EY, Maliszewski CR. Soluble IL-4 receptor inhibits airway inflammation following allergen challenge in a mouse model of asthma. *J Immunol* 2000; **164**:1086–95.
36 Tomkinson A, Duez C, Cieslewicz G *et al.* A murine IL-4 receptor antagonist that inhibits IL-4- and IL-13-induced responses prevents antigen-induced airway eosinophilia and airway hyperresponsiveness. *J Immunol* 2001; **166**:5792–800.
37 Grunewald SM, Werthmann A, Schnarr B *et al.* An antagonistic IL-4 mutant prevents type I allergy in the mouse: inhibition of the IL-4/IL-13 receptor system completely abrogates humoral immune response to allergen and development of allergic symptoms *in vivo*. *J Immunol* 1998; **160**:4004–9.
38 Hayashi T, Yasutomi Y, Hasegawa K *et al.* Interleukin-4-expressing plasmid DNA inhibits reovirus type-2-triggered autoimmune insulitis in DBA/1 J suckling mice. *Int J Exp Pathol* 2003; **84**:101–6.
39 Ruzicka T, Gluck S. Cutaneous histamine levels and histamine releasability from the skin in atopic dermatitis and hyper-IgE-syndrome. *Arch Dermatol Res* 1983; **275**:41–4.
40 Horsmanheimo L, Harvima IT, Jarvikallio A *et al.* Mast cells are one major source of interleukin-4 in atopic dermatitis. *Br J Dermatol* 1994; **131**:348–53.
41 Gibbs BF, Wierecky J, Welker P *et al.* Human skin mast cells rapidly release preformed and newly generated TNF-alpha and IL-8 following stimulation with anti-IgE and other secretagogues. *Exp Dermatol* 2001; **10**:312–20.
42 Leung DY. Atopic dermatitis: immunobiology and treatment with immune modulators. *Clin Exp Immunol* 1997; **107** (Suppl. 1):25–30.
43 Schleimer RP, Sterbinsky SA, Kaiser J *et al.* IL-4 induces adherence of human eosinophils and basophils but not neutrophils to endothelium. Association with expression of VCAM-1. *J Immunol* 1992; **148**:1086–92.
44 Mistry AR, Falciola L, Monaco L *et al.* Recombinant HMG1 protein produced in Pichia pastoris: a nonviral gene delivery agent. *BioTechniques* 1997; **22**:718–29.
45 Gurunathan S, Klinman DM, Seder RA. DNA vaccines: immunology, application, and optimization. *Annu Rev Immunol* 2000; **18**:927–74.

J. Comp. Path. 2009, Vol. 140, 212–216

ELSEVIER
www.elsevier.com/locate/jcpa

SHORT PAPER

Acute Megakaryocytic Leukaemia (AMKL)-like Disease in a Cynomolgus Monkey (*Macaca fascicularis*)

S. Okabayash*,†, C. Ohno* and Y. Yasutomi†

* *The Corporation for Production and Research of Laboratory Primates and † Tsukuba Primate Research Center, National Institute of Biomedical Innovation, Hachimandai 1-1, Tsukuba-shi, Ibaraki 305-0843, Japan*

Summary

A 5-year-old male cynomolgus monkey (*Macaca fascicularis*) with a clinical history of bleeding tendency, severe anaemia, thrombocytopenia and elevated serum concentration of liver-related enzymes was examined *post mortem*. Ecchymotic haemorrhages were present on the left eyelid and forehead. The liver, kidney and spleen were markedly enlarged and the kidneys had capsular petechiae. Microscopically, numerous atypical cells resembling myeloid cells were observed in the bone marrow, and myelofibrosis was present. Atypical cells were also present in the blood vessels of the liver, kidney, spleen, lymph nodes, lung, heart, bladder, adrenal gland and brain. Some neoplastic cells had oval or pleomorphic macronuclei and others were multinucleated. Immunohistochemically, the majority of the neoplastic cells had granular cytoplasmic expression of the megakaryocyte-associated antigens Von Willebrand Factor and CD61-IIIa, but were negative for myeloperoxidase. A diagnosis of acute megakaryocytic leukaemia (AMKL)-like disease was made. This would appear to be the first report of AMKL-like disease in non-human primates. This monkey was infected with simian retrovirus type D and it is possible that this viral infection was associated with the development of neoplasia.

Keywords: acute megakaryocytic leukaemia; cynomolgus monkey; immunohistochemistry; simian retrovirus type D

Haematological malignancy has been infrequently documented in monkeys infected by the simian immunodeficiency virus (SIV) (Fortgang *et al.*, 2000). Simian T-cell leukaemia virus (STLV) is also linked to the development of simian T-cell malignancies that closely resemble human T-lymphotropic virus (HTLV) associated leukaemia and lymphoma (Hubbard *et al.*, 1993). Furthermore, simian retrovirus type D (SRV/D) is a common cause of simian acquired immunodeficiency syndrome (SAIDS), a fatal immunosuppressive disease of macaques. SRV/D-infected monkeys may develop lymphadenopathy, splenomegaly, anaemia, bone marrow hyperplasia, lymphoid depletion, neutropenia, weight loss, diarrhoea or malignant neoplasia (Guzman *et al.*, 1999). Although a number of clinical and pathological studies have described lymphoma in non-human primates (Hubbard *et al.*, 1993; Paramastri *et al.*, 2002), there are no reports of myeloid leukaemia in these animals. The present report describes the first case of acute megakaryocytic leukaemia (AMKL)-like disease in a non-human primate.

A 5-year-old male cynomolgus monkey (*Macaca fascicularis*) was housed in the Tsukuba Primate Research Center (TPRC) in an individual cage and maintained according to the National Institute of Biomedical Innovation rules and guidelines for experimental animal welfare. On routine haematological examination, the animal was found to have mild anaemia (red blood cells [RBC] 4.28×10^{12}/l; reference range $5.55–6.68 \times 10^{12}$/l; haemoglobin [Hb] 99 g/l; reference range 105–125 g/l; haematocrit [HCT] 32.7%; reference range 35.4–41.4%) and severe thrombocytopenia (platelets [PLT] 27×10^9/l; reference range $195–339 \times 10^9$/l). The number of white blood cells (WBC) was normal (6.9×10^9/l; reference

Correspondence to: S. Okabayash e-mail: okarin@primate.or.jp.

0021-9975/$ - see front matter
doi:10.1016/j.jcpa.2008.11.007

range 4.2–9.2 × 10^9/l). Although the animal care staff regularly monitored the health of the animal, at this time no clinical signs were observed. Repeat haematological examinations were performed one and four weeks later, but there was no progression of the anaemia and thrombocytopenia was not present on these occasions. The monkey continued to have normal appetite, faeces and activity.

Three months after the initial haematological examination a spot of blood was detected under the monkey's cage. At this time the animal displayed clinical signs including emaciation, pallor of mucous membranes and haemorrhage on the cutaneous side of one eyelid. Haematological examination revealed severe anaemia (RBC 1.66 × 10^{12}/l, Hb 39 g/l, HCT 13.3%) and thrombocytopenia (PLT 28 × 10^9/l). The WBC count was normal (4.1 × 10^9/l). Serum biochemical examination revealed elevation in the concentration of aspartate aminotransferase (AST, 176 U/l; reference range 31–47 U/l); alanine aminotransferase (ALT, 303 U/l; reference range 21–65 U/l); lactate dehydrogenase (LDH, 7660 U/l; reference range 292–975 U/l), and C reactive protein (CRP, 12.8 mg/l; reference range 0.3–1.7 mg/l).

Cynomolgus monkeys in the TPRC breeding colony are SIV and STLV negative, but most are infected by SRV/D (Hara *et al.*, 2005). The animal described here was seronegative for SRV/D antibody by western blotting, but tested positive by polymerase chain reaction (PCR) for the detection of virus genetic material, consistent with current viraemia. On the basis of the clinical and laboratory data, haematological malignancy was suspected.

The monkey was deeply anaesthetized with a lethal dose of pentobarbital and necropsy examination was performed. Ecchymoses were noted on the left eyelid and forehead. The liver was markedly enlarged and the gallbladder was distended. The kidneys were enlarged, pale red-brown in colour and had capsular petechiation. The spleen was also enlarged, but there were no distinct lymphoid follicles on the cut surface. A dark red nodule (1 cm diameter) was present within each of the inferior lobes of the lung. The femoral bone marrow had a brownish-red appearance.

Tissues were fixed in 10% neutral buffered formalin, processed routinely and embedded in paraffin wax. Sections (3 μm) were stained with haematoxylin and eosin (HE), periodic acid-Schiff (PAS) and Masson's trichrome stains. Microscopically, many atypical cells resembling myeloid cells were observed in the bone marrow and the blood vessels of the liver, kidney, spleen, lymph nodes, lung, heart, bladder, adrenal gland and brain. Some hepatic and renal vessels contained neoplastic emboli (Fig. 1). There was extensive infiltration of the liver, kidneys and adrenal

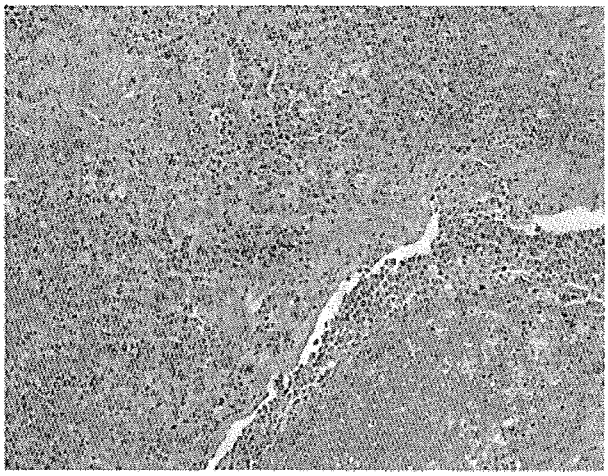

Fig. 1. Extensive infiltration of neoplastic cells into the hepatic parenchyma with associated degeneration and necrosis. A tumour embolus has formed in the central vein. HE. ×100.

glands by the same neoplastic population, with associated parenchymal degeneration or necrosis. Neoplastic cells were present in the spleen and lymph nodes, and in both tissues there was atrophy of lymphoid follicles. Sternal and femoral bone marrow contained many abnormal blast cells, with a marked reduction in normal haemopoietic tissue.

The neoplastic cells were generally poorly differentiated, with a medium-sized round nucleus, dense nuclear chromatin and either scant or abundant cytoplasm. Some larger cells had oval or pleomorphic macronuclei, whilst others were multinucleated, with a lower nuclear to cytoplasmic ratio (Fig. 2). There

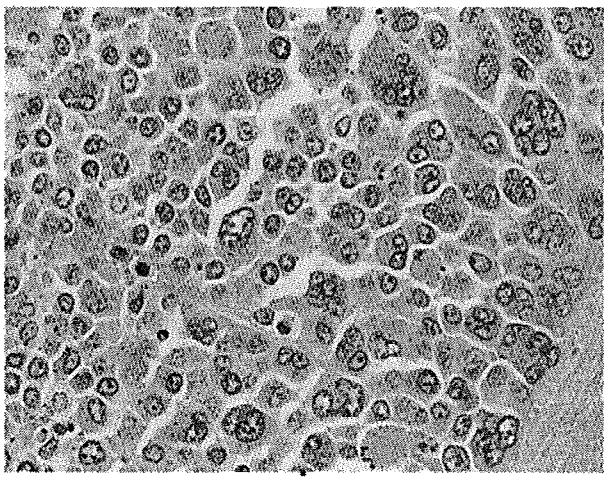

Fig. 2. Neoplastic cells within the liver. These vary greatly in size and are generally 2–3 times larger than normal lymphocytes. The majority of cells have large, round to oval nuclei with stippled chromatin and abundant cytoplasm. Some cells have macronuclei and others are multinucleated, with a lower nucleus to cytoplasmic ratio. HE. ×400.

were numerous abnormal mitoses. The majority of blast cells did not stain with PAS, but occasional individual cells were weakly stained. Masson's trichrome staining demonstrated severe fibrosis of the bone marrow (Fig. 3).

To further identify the neoplastic cells, immunohistochemical studies of femoral bone marrow, liver and kidney were performed. Sections were dewaxed, pre-treated with 0.5% H_2O_2 in methanol and then subjected to antigen retrieval with citric acid buffer (pH 6.0) and heating in an autoclave for 10 min at 121°C. Sections were then incubated with primary antibody overnight at 4°C. The primary antibodies employed were rabbit polyclonal antibodies specific for myeloperoxidase (Novocastra Laboratories, Newcastle, UK; 1 in 150 dilution); Von Willebrand Factor (Dako Cytomation, Denmark; 1 in 400 dilution); CD3 (Dako, 1 in 100 dilution); lysozyme (clone EC 3.2.1.17, Dako; 1 in 400 dilution) and monoclonal mouse antibodies specific for CD235a (clone JC159, Dako; 1 in 200 dilution); CD61-IIIa (cloneY2/51, Dako; 1 in 100 dilution); CD20 (clone L26, Dako; 1 in 100 dilution); HLA-DR alpha-chain (clone TAL.1B5, Dako; 1 in 40 dilution) and CD68 (clone KP1, Dako; 1 in 100 dilution). Following brief washes with buffer, the sections were incubated with the EnVision™ + Dual Link-HRP system (Dako) as secondary stage for 30 min. Labelling was "visualized" by treating the sections with the chromogen 3-3′-diaminobenzidine tetroxide (Dojin Kagaku, Japan) and H_2O_2. The sections were then counterstained with haematoxylin.

The majority of the neoplastic cells had granular cytoplasmic expression of the megakaryocyte-associated antigens Von Willebrand Factor (Fig. 4) and CD61-IIIa, but were negative for all other markers. On the basis of these findings, a diagnosis of AMKL (M7)-like disease with myelofibrosis was made. The neoplastic cells in AMKL often have granular cytoplasmic PAS staining when examined in a blood or a bone marrow smear (Wu *et al.*, 1996; Shukla *et al.*, 2004). The absence of significant PAS staining in the cells of the present case may relate to the formalin fixation process.

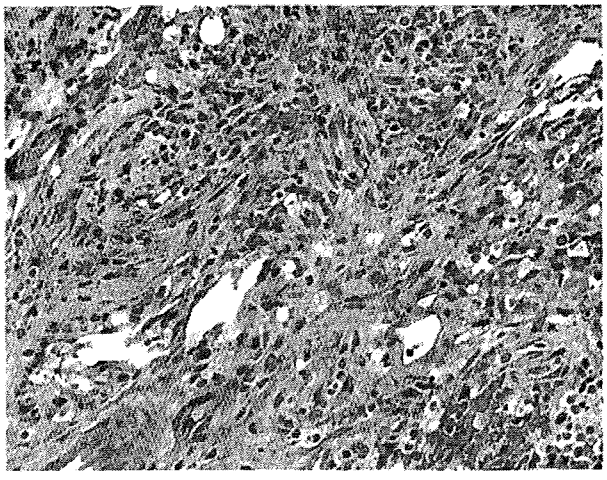

Fig. 3. Marked fibrosis (blue staining) is present within the bone marrow and admixed with neoplastic cells. Masson's trichrome. ×200.

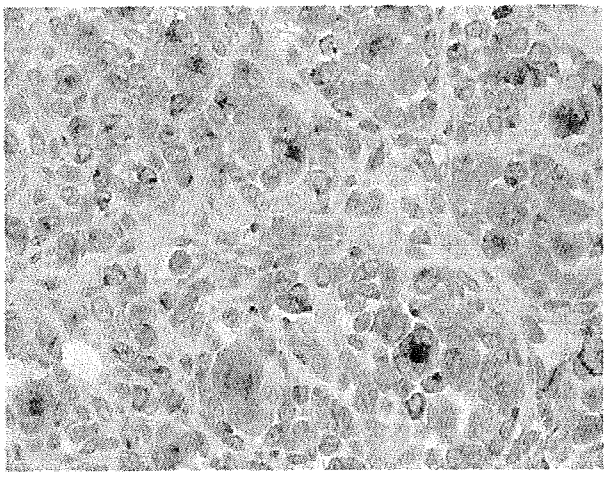

Fig. 4. Expression of Von Willebrand Factor by neoplastic cells within the bone marrow. IHC. ×400.

AMKL was first described as a subtype of acute myeloid leukaemia (AML) (von Boros and Korenyi, 1931) and was incorporated into the French–American–British (FAB) classification of AML as M7 (Bennett *et al.*, 1985). AMKL is rare, accounting for 3–5% of all human AML (Brunning *et al.*, 2001), but there is a higher incidence in children, partly due to an association with Down's syndrome (Athale *et al.*, 2001; Paredes-Aguilera *et al.*, 2003). Although AMKL is well characterized in man (Koike, 1984; Akahoshi *et al.*, 1987), in animals it has been reported only in the dog and cat (Colbatzky and Hermanns, 1993). Disrupted haematopoiesis leads to cytopenia, particularly thrombocytopenia, which becomes manifest as cutaneous petechiae, epistaxis and bleeding gums. In leukaemic patients there is often elevation of serum LDH concentration (Ferrara and Mirto, 1996). Since megakaryocytes, which store various growth factors in their alpha granules, are known to be involved in the pathogenesis of myelofibrosis, AMKL is frequently accompanied by myelofibrosis (Terui *et al.*, 1990). AMKL typically has a more guarded prognosis than other types of leukaemia (Athale *et al.*, 2001).

Differential diagnoses for AMKL include minimally differentiated AML (M0), pure erythroid

leukaemia (M6b) and acute lymphocytic leukaemia (ALL). M0, M6b and ALL are all generally negative for expression of myeloperoxidase in immunohistochemistry (IHC), as is AMKL. The neoplastic cells in AMKL occasionally have a lymphoblast-like appearance similar to M0 and ALL (Brunning *et al.*, 2001). Furthermore, neoplastic multinucleate cells are observed in both M6b and AMKL, and are often positively stained by PAS (Brunning *et al.*, 2001). Megakaryoblasts do not express myeloperoxidase, but are labelled by one or more of the megakaryocyte-associated antigens CD41, CD61 and Von Willebrand Factor (Brunning *et al.*, 2001; Daniel and Arber, 2001). The cytological and immunohistochemical features of the neoplastic population in the present case were not consistent with M0, M6b or ALL.

Further differential diagnoses for AMKL with myelofibrosis, as described in the present case, include acute panmyelosis with myelofibrosis (APMF), blastic transformation of chronic myeloid leukaemia (CML) or idiopathic myelofibrosis (IMF). APMF is characterized by multi-lineage myeloid proliferation, with a less numerous population of blast cells than in acute megakaryoblastic leukaemia (Orazi *et al.*, 2005). The cells in APMF do not express megakaryocyte-related antigens, which is inconsistent with the findings in the present case. CML is a clonal bone marrow stem cell disorder with proliferation of mature granulocytes (Travis *et al.*, 1987; Bourantas *et al.*, 1998) whereas IMF is a clonal myeloproliferative disorder that is characterized by abnormal deposition of collagen within the bone marrow (Hirose *et al.*, 2001). Human patients with CML or IMF also develop terminal blastic transformation, and these blast cells have frequently been identified as megakaryoblasts (Travis *et al.*, 1987; Bourantas *et al.*, 1998; Hirose *et al.*, 2001). Although the present case most likely represents AMKL with myelofibrosis, it is difficult to entirely exclude the alternative interpretation of blastic transformation of CML or IMF. For this reason, the present case has been described as an AMKL (M7)-like disease.

To our knowledge, this is the first case of spontaneously arising AMKL-like disease in non-human primates. The affected monkey had SRV/D infection, which may have contributed to the development of the neoplastic disease (Guzman *et al.*, 1999). Alternatively, a genetic mechanism may be proposed as humans with Down's syndrome have predisposition to the development of AMKL associated with a somatic mutation in the gene encoding the GATA1 transcription factor protein (Shimizu *et al.*, 2008). Further cases of such leukaemia in non-human primates should be subject to genetic investigation.

Acknowledgments

This study was supported by the Tsukuba Primate Research Center, National Institute of Biomedical Innovation, Japan.

References

Akahoshi, M., Oshimi, K., Mizoguchi, H., Okada, M., Enomoto, Y. and Watanabe, Y. (1987). Myeloproliferative disorders terminating in acute megakaryoblastic leukemia with chromosome 3q26 abnormality. *Cancer*, **60**, 2654–2661.

Athale, U. H., Razzouk, B. I., Raimondi, S. C., Tong, X., Behm, F. G., Head, D. R., Srivastava, D. K., Rubnitz, J. E., Bowman, L., Pui, C. H. and Ribeiro, R. C. (2001). Biology and outcome of childhood acute megakaryoblastic leukemia: a single institution's experience. *Blood*, **97**, 3727–3732.

Bennett, J. M., Catovsky, D., Daniel, M. T., Flandrin, G., Galton, D. A., Gralnick, H. R. and Sultan, C. (1985). Criteria for the diagnosis of acute leukemia of megakaryocyte lineage (M7). A report of the French–American–British Cooperative Group. *Annals of Internal Medicine*, **103**, 460–462.

von Boros, J. and Korenyi, A. (1931). Uber einen fall von akuter megakaryocyblasten-leukamie, zugleich einige bemerkungen zum problem der akuten leukemie. *Zeitschrift für Klinische Medizin*, **118**, 679–718.

Bourantas, K. L., Repousis, P., Tsiara, S., Christou, L., Konstantinidou, P. and Bai, M. (1998). Chronic myelogenous leukemia terminating in acute megakaryoblastic leukemia. Case report. *Journal of Experimental and Clinical Cancer Research*, **17**, 243–245.

Brunning, R. D., Matutes, E., Flandrin, G., Vardiman, J., Bennett, J., Head, D. and Harris, N. L. (2001). Acute myeloid leukemias. Pathology and genetics of tumours of haematopoietic and lymphoid tissues. In: *World Health Organization Classification of Tumors*, E. S. Jaffe, N. L. Harris, H. Stein and J. W. Vardiman, Eds, IARC Press, Lyon, pp. 77–105.

Colbatzky, F. and Hermanns, W. (1993). Acute megakaryoblastic leukemia in one cat and two dogs. *Veterinary Pathology*, **30**, 186–194.

Daniel, A. and Arber, M. D. (2001). Realistic pathologic classification of acute myeloid leukemias. *American Journal of Clinical Pathology*, **115**, 552–560.

Ferrara, F. and Mirto, S. (1996). Serum LDH value as a predictor of clinical outcome in acute myelogenous leukaemia of the elderly. *British Journal of Haematology*, **92**, 627–631.

Fortgang, I. S., Didier, P. J. and Levy, L. S. (2000). B-cell leukemia in a rhesus macaque (*Macaca mulatta*) infected with simian immunodefieiency virus. *Leukemia and Lymphoma*, **37**, 657–662.

Guzman, R. E., Kerlin, R. L. and Zimmerman, T. E. (1999). Histologic lesions in cynomolgus monkeys (*Macaca fascicularis*) naturally infected with simian retrovirus type D: comparison of seropositive, virus-positive, nd uninfected animals. *Toxicologic Pathology*, **27**, 672–677.

Hara, M., Kikuchi, T., Ono, F., Takano, J., Ageyama, N., Fujimoto, K., Terao, K., Baba, T. and Mukai, R. (2005). Survey of captive cynomolgus macaque colonies for SRV/D infection using polymerase chain reaction assays. *Comparative Medicine*, **55**, 145–149.

Hirose, Y., Masaki, Y., Shimoyama, K., Sugai, S. and Nojima, T. (2001). Granulocytic sarcoma of megakaryoblastic differentiation in the lymph nodes terminating as acute megakaryoblastic leukemia in a case of chronic idiopathic myelofibrosis persisting for 16 years. *European Journal of Haematology*, **67**, 194–198.

Hubbard, G. B., Moné, J. P., Allan, J. S., Davis, K. J., 3rd, Leland, M. M., Banks, P. M. and Smir, B. (1993). Spontaneously generated non-Hodgkin's lymphoma in twenty-seven simian T-cell leukemia virus type 1 antibody-positive baboons (*Papio species*). *Laboratory Animal Science*, **43**, 301–309.

Koike, T. (1984). Megakaryoblastic leukemia: the characterization and identification of megakaryoblasts. *Blood*, **64**, 683–692.

Orazi, A., O'Malley, D. P., Jiang, J., Vance, G. H., Thomas, J., Czader, M., Fang, W., An, C. and Banks, P. M. (2005). Acute panmyelosis with myelofibrosis: an entity distinct from acute megakaryoblastic leukemia. *Modern Pathology*, **18**, 603–614.

Paramastri, Y. A., Wallace, J. M., Salleng, K. J., Wilkinson, L. M., Malarkey, D. E. and Cline, J. M. (2002). Intracranial lymphomas in simian retrovirus-positive *Macaca fascicularis*. *Veterinary Pathology*, **39**, 399–402.

Paredes-Aguilera, R., Romero-Guzman, L., Lopez-Santiago, N. and Trejo, R. A. (2003). Biology, clinical, and hematologic features of acute megakaryoblastic leukemia in children. *American Journal of Hematology*, **73**, 71–80.

Shimizu, R., Engel, J. D. and Yamamoto, M. (2008). GATA1-related leukaemias. *Nature Reviews Cancer*, **8**, 279–287.

Shukla, J., Rai, S. and Singh, V. P. (2004). Acute megakaryoblastic leukaemia: a clinico-haematological profile of five cases. *Indian Journal of Pathology and Microbiology*, **47**, 266–268.

Terui, T., Niitsu, Y., Mahara, K., Fujisaki, Y., Urushizaki, Y., Mogi, Y., Kohgo, Y., Watanabe, N., Ogura, M. and Saito, H. (1990). The production of transforming growth factor-beta in acute megakaryoblastic leukemia and its possible implications in myelofibrosis. *Blood*, **75**, 1540–1548.

Travis, W. D., Li, C. Y., Banks, P. M. and Nichols, W. L. (1987). Megakaryoblastic transformation of chronic granulocytic leukemia. *Cancer*, **60**, 193–200.

Wu, C. D., Medeiros, L. J., Miranda, R. N., Mark, H. F. and Rintels, P. (1996). Chronic myeloid leukemia manifested during megakaryoblastic crisis. *Southern Medical Journal*, **89**, 422–427.

[*Received, September 5th, 2008*
Accepted, November 19th, 2008]

Parasitol Res (2009) 105:929–937
DOI 10.1007/s00436-009-1480-3

ORIGINAL PAPER

DNA characterization of simian *Entamoeba histolytica*-like strains to differentiate them from *Entamoeba histolytica*

Jun-ichiro Takano · Hiroshi Tachibana · Miyoko Kato · Toyoko Narita · Tetsuo Yanagi · Yasuhiro Yasutomi · Koji Fujimoto

Received: 27 March 2009 / Accepted: 8 May 2009 / Published online: 27 May 2009

Abstract Two simian *Entamoeba histolytica*-like strains, EHMfas1 and P19-061405, have been suggested to represent a new species based on genetic characterization. Sequence analyses of the hexokinase, glucose phosphate isomerase, and phosphoglucomutase genes supported the previous findings of isoenzyme analyses demonstrating a new zymodeme pattern. Phylogenetic studies of 18S rDNA, 5.8S rDNA, the chaperonin 60 gene, and the pyridine nucleotide transhydrogenase gene showed original clusters of simian *E. histolytica*-like strains below or near *E. histolytica*, respectively. Comparative studies of the chitinase and the serine-rich *E. histolytica* protein genes and locus 1–2 region revealed that most mutated units were shared among the simian *E. histolytica*-like strains. The similarities of each of the repeating units within the simian *E. histolytica*-like strains or *E. histolytica* and the differences of those between the both might be generated by concerted evolution. Our results indicate that EHMfas1 and P19-061405 should be considered to be the same species, despite that they were isolated from different monkey species and different habitats. Simian *E. histolytica*-like amebas may be endemic to macaque monkeys, as a counterpart to *E. histolytica* in humans, and should be differentiated from *E. histolytica* by the revival name *Entamoeba nuttalli*, as proposed for P19-061405.

J.-i. Takano (✉) · M. Kato · T. Narita · K. Fujimoto
The Corporation for Production and Research
of Laboratory Primates,
1-1 Hachimandai,
Tsukuba, Ibaraki 305-0843, Japan
e-mail: takano@primate.or.jp

H. Tachibana
Department of Infectious Diseases,
Tokai University School of Medicine,
143 Shimokasuya,
Isehara, Kanagawa 259-1193, Japan

T. Yanagi
Animal Research Center for Tropical Infections,
Institute of Tropical Medicine, Nagasaki University,
1-12-4 Sakamoto,
Nagasaki, Nagasaki 852-8523, Japan

Y. Yasutomi
Tsukuba Primate Research Center,
National Institute of Biomedical Innovation,
1-1 Hachimandai,
Tsukuba, Ibaraki 305-0843, Japan

Introduction

Entamoeba histolytica causes amoebic colitis and liver abscess, and amoebiasis is one of the most important parasitic diseases in humans. In non-human primates, several cases of *E. histolytica* or *E. histolytica*-like organism infections have been identified by isoenzyme analysis, monoclonal antibody test, or PCR (Tachibana et al. 1990; Verweij et al. 2003; Takano et al. 2005; Tachibana et al. 2007; Suzuki et al. 2007). One of the simian *E. histolytica*-like strains, EHMfas1, has been isolated from a healthy cynomolgus monkey (*Macaca fascicularis*) and identified using species-specific PCR for *E. histolytica* and antigen-capture ELISA (Takano et al. 2005). Another simian *E. histolytica*-like strain, P19-061405, has been isolated from a rhesus monkey (*Macaca mulatta*). Furthermore, the virulence of P19-061405 has also been confirmed by experimental infection of hamsters (Tachibana et al. 2007).

These two simian *E. histolytica*-like strains were suggested to be a new species, because EHMfas1 exhibits differences in the 16S-like small subunit ribosomal RNA

(18S rDNA), chitinase and SREHP genes, and P19-061405 exhibits differences in several DNA sequences, including the 18S rDNA and SREHP genes (Takano et al. 2007; Tachibana et al. 2007). It has been proposed that P19-061405 should be distinguished from *E. histolytica* by revival of the name *Entamoeba nuttalli* (Castellani 1908) that was the first reported *E. histolytica*-like species found in a liver abscess of a monkey (Tachibana et al. 2007). Isoenzyme analyses of these two simian *E. histolytica*-like strains have demonstrated a new and similar zymodeme pattern.

In this study, we compared these two simian *E. histolytica*-like strains based on DNA loci that were used for isoenzyme analysis, phylogenetic investigation, and genotyping to determine the similarity between the simian *E. histolytica*-like strains and the differences between simian *E. histolytica*-like amebas and *E. histolytica*.

Materials and methods

Simian *E. histolytica*-like strains

Trophozoites of the EHMfas1 strain were cultured monoxenically with *Crithidia fasciculata* and axenically in BI-S-33 medium supplemented with 15% adult bovine serum at 37°C (Diamond et al. 1978) and then cloned by limiting dilution, followed by examination using microscopy. Trophozoites of the cloned P19-061405 strain were also axenically cultured in BI-S-33 medium (Tachibana et al. 2007).

Hepatic inoculation of hamsters

Hamsters were inoculated with trophozoites of the EHMfas1 that had been cultured monoxenically with *C. fasciculata* as described by Tachibana et al. (2007).

DNA preparation and sequencing

Total genomic DNA from each cloned trophozoite was extracted using a QIAamp DNA Stool Mini Kit (Qiagen) or a DNeasy tissue kit (Qiagen) according to the manufacturer's instructions.

The genomic DNA from cloned trophozoites was amplified using the primers listed in Table 1. PCR was conducted in a 50 μl reaction mixture containing 2 μl of extracted DNA and 0.1 μg/μl bovine serum albumin using PrimeSTAR Max DNA polymerase (Takara). A total of 35 cycles of PCR were performed, as follows: denaturation at 98°C for 10 s, annealing at 62°C (for pyridine nucleotide transhydrogenase (PNT)) or 56°C (for other genes) for 5 s, and extension at 72°C for 15 s.

Amplified genes for hexokinase (HXK), glucose-6-phosphate isomerase (GPI), and phosphoglucomutase (PGM) from EHMfas1 and chaperonin 60 (Cpn60) were cloned from P19-061405 using a Zero Blunt TOPO PCR cloning kit for sequencing (Invitrogen). Each clone was subjected to sequencing using a BigDye Terminator v3.1 Cycle Sequencing Kit (Applied Biosystems) on an ABI PRISM 3100-Avant Genetic Analyzer (Applied Biosystems), according to the manufacturer's instructions. PCR products for 5.8S rDNA with internal-transcribed spacer (ITS) 1 and ITS 2, Cpn60, and PNT, locus 1–2 from EHMfas1 and PNT, and chitinase and locus 1–2 from P19-061504 were sequenced directly. Sequence data were analyzed using DNASIS Pro ver. 2.08 (Hitachi software). The GenBank accession numbers of the sequences used for comparison with each gene are shown in Figs. 1, 2, 3, and 4.

Phylogenetic analysis

Analysis and multiple alignments of DNA sequences of 18S rDNA, 5.8S rDNA with ITS 1 and ITS 2, Cpn60, and PNT were performed with ClustalX (Thompson et al. 1997), and the phylogenetic trees were constructed using the neighbor-joining method (Saitou and Nei 1987).

Nucleotide sequence accession numbers

The nucleotide sequence data reported here have been submitted to the GenBank/EMBL/DDBJ databases under accession numbers AB454548 to AB454559 and AB480745.

Results

Virulency of EHMfas1 in hamster

EHMfas1 was monoxenically cultured with *C. fasciculata* and inoculated into the livers of hamsters. Liver abscesses were observed in all hamsters at 7 days after inoculation. The presence of trophozoites in the peripheral regions of abscesses in the livers was confirmed in PAS stained tissue slides. No abscesses were observed in the control hamsters, inoculated with *C. fasciculata* alone.

Analysis of zymodeme-related genes

Two HXK genes of EHMfas1 were amplified from the cloned EHMfas1 trophozoites and sequenced after molecular cloning. The calculated molecular masses and isoelectric points (p*I*) were 49.7 kDa and 5.38 in HXK 1 and 49.4 kDa and 4.99 in HXK 2. The deduced amino-acid sequences were compared with those of P19-061405

Table 1 Primers used in this study

Locus	Direction (name of primer)	Sequence (5′-3′)	Reference
HXK	S	ATG CAA GAA ATC ATT GAT CAA TTT	Tachibana et al. 2007
HXK1	AS	TTA GTG TTT ACA TGC AAC AGC A	
HXK2	AS	TTA TTG TTT GCA TGC AAC AGC A	
GPI	S	ATG TTA CCA ACT CTT CCT GAA T	Tachibana et al. 2007
	AS	TTA GTT TTT TCT CAT ATC TTT AAC A	
PGM	S (PGMoutS)	TCG TTG AAC CAG ATC AGT GC	Genome database region on scaffold 00005[a]
	AS (PGMoutAS)	AAG CTT CTC TGG ATG GTG TTG	
ITS1, 5.8S	S (P1)	AGG TGA ACC TGC GGA AGG ATC ATT A	Som et al. 2000
ITS2	AS (P2)	TCA TTC GCC ATT ACT TAA GAA ATC ATT GTT	
Cpn60	S (CpnOf1)	GTT GAA CTT TTC ATA AGG TTG TTT GA	Genome database region on scaffold 00015[a]
	AS (CpnOr1)	CAA AAA TGG GCA GAT GAA CA	
PNT	S (PNT-A)	GTA GGA CTT GCA GCA GTA TT	Bakatselou et al. 2003
	AS (PNT-B)	GGT AAT CTT CCT GCA ACT GG	
Chitinase	S	GGA ACA CCA GGT AAA TGT ATA	Ghosh et al. 2000
	AS	TCT GTA TTG TGC CCA ATT	
Locus 1–2	S (R1)	CTG GTT AGT ATC TTC GCC TGT	Zaki et al. 2002
	AS (R2)	CTT ACA CCC CCA TTA ACA AT	

S sense, *AS* anti-sense

[a] Present study

(GenBank accession numbers: AB282663 for HXK 1 and AB282664 for HXK 2). Glu^{13} and Asn^{32} in HXK 1 of P19-061405 were changed to Gly and Asp, respectively, in HXK 1 of EHMfas1. HXK 2 of EHMfas1was identical to that of P19-061405. The p*I*s for HXK 1 and HXK 2 of EHMfas1 were consistent with those of P19-061405 (Tachibana et al. 2007).

The GPI gene of EHMfas1 was also amplified and sequenced after molecular cloning, and only one GPI gene was obtained from 16 clones. The calculated molecular mass and p*I* for GPI of EHMfas1, 61.4 kDa and 6.60, were also consistent with those of P19-061405. In the deduced amino-acid sequence, Val^{232} in GPI 1 of P19-061405 (GenBank accession number: AB282665) was changed to Ile, and Val^{330} in the GPI 2 of P19-061405 (GenBank accession number: AB282666) was changed to Ala in EHMfas1.

One PGM gene from EHMfas1 was detected in clones from EHMfas1. The calculated molecular mass and p*I* for PGM were 60.8 kDa and 5.99, respectively. In the deduced amino-acid sequence of PGM from EHMfas1, there were four and 13 differences compared with *E. histolytica* (GenBank accession number: Y14444) and *Entamoeba dispar* (GenBank accession number: Y14445), respectively. Although the isoenzyme pattern of PGM in EHMfas1 was identical to *E. dispar*, the amino-acid sequences of PGM in EHMfas1 were more similar to *E. histolytica* than *E. dispar*.

Analyses and phylogenic studies of ribosomal RNA genes and mitosome genes

Comparison of the 18S rDNA sequences reported for EHMfas1 (Takano et al. 2007) and P19-061405 (Tachibana et al. 2007) showed a difference of 0.1% (two of 1,945). A reconstructed phylogenetic tree showed the original cluster of simian *E. histolytica*-like strains beside the *E. histolytica* branch (Fig. 1a). The 5.8S rDNA, with ITS 1 and 2 regions of EHMfas1, was sequenced directly. Comparison of this region of EHMfas1 and P19-061405 (Tachibana et al. 2007) showed no differences throughout the length. The constructed phylogenetic tree of this region also showed that the simian isolates were located beside the *E. histolytica* branch (Fig. 1b). The Cpn60 and PNT genes of EHMfas1 and P19-061405 were directly sequenced. Although DNAs were extracted from cloned trophozoites, obvious mixed sequences were confirmed by direct sequencing of Cpn60 gene from P19-061405. The Cpn60 gene from P19-061405 was cloned, and we obtained two Cpn60 gene alleles from six clones. In the nucleotide sequence of Cpn60 from EHMfas1, five and four differences were present compared with P19-061405 alleles 1 and 2, respectively. In the deduced amino-acid sequence, all Cpn60 from EHMfas1 and P19-061405 were consistent with *E. histolytica*. The phylogenetic relationship of the Cpn60 genes among *Entamoeba* species was also reconstructed (Fig. 1c). In

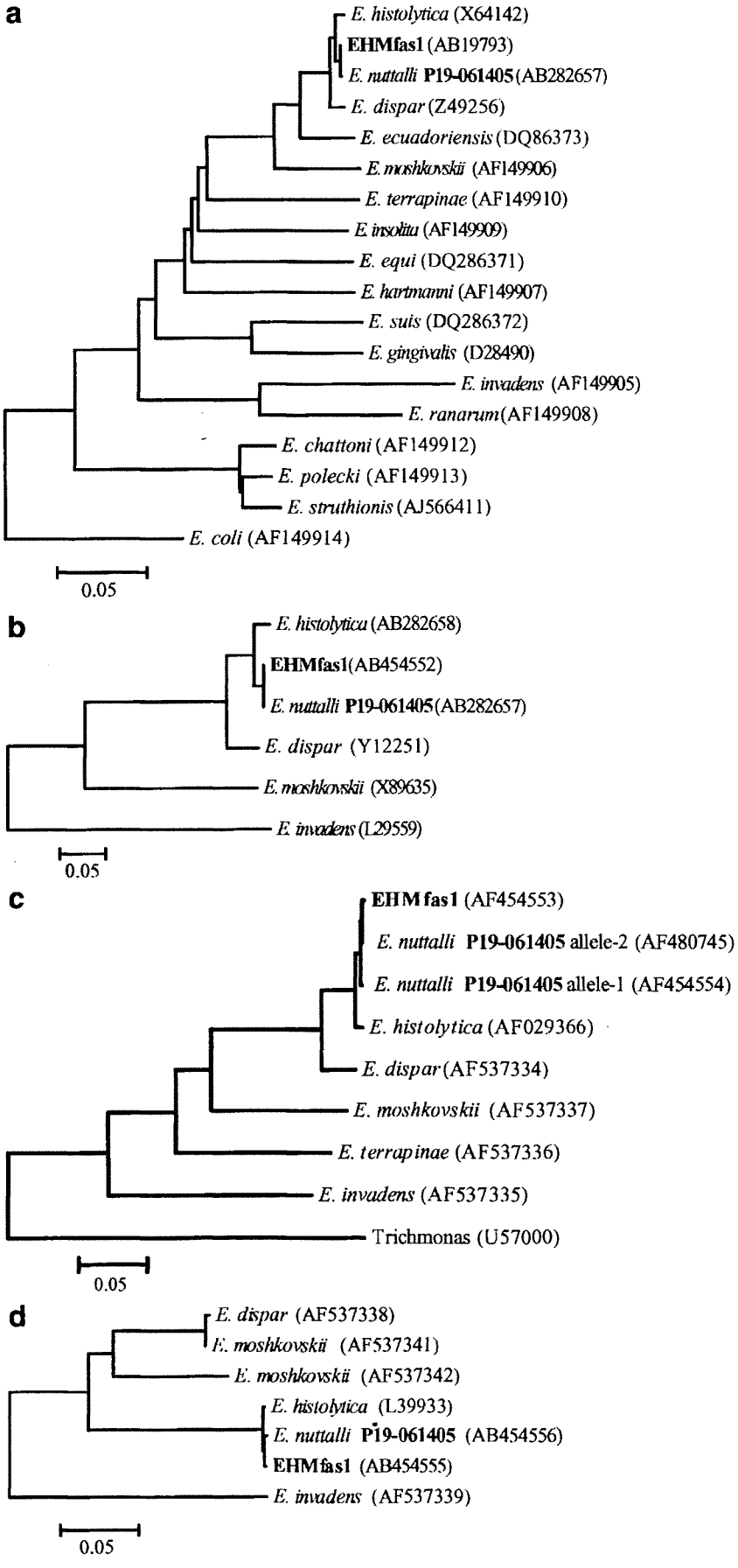

Fig. 1 Phylogenetic relationships among simian *E. histolytica*-like strains and other *Entamoeba* species. 18S rDNA sequences (**a**), 5.8S rDNA with ITS1 and ITS2 sequences (**b**), the Cpn60 gene sequences (**c**), and the PNT gene sequences (**d**). Branch lengths are proportional to estimated number of substitutions per site, which represent the evolutional distance

the reconstructed phylogenetic tree of the Cpn60 genes, the cluster of simian *E. histolytica*-like strains was located under the *E. histolytica* branch. PNT gene sequences were also compared between EHMfas1 and P19-061405, and a difference of 0.23% (one of 432) was evident. *E. histolytica*, EHMfas1 and P19-061405, was categorized in the same cluster (Fig. 1d).

Comparison of polymorphic loci: the chitinase gene, SREHP gene, and locus 1–2

The chitinase gene of P19-061405 was directly sequenced and compared with the reported sequences of EHMfas1, KU3 (genotype A) and KU15 (genotype D) of *E. histolytica* (Fig. 2; de la Vega et al. 1997; Ghosh et al. 2000; Haghighi et al. 2002, 2003). Each unit of the nucleotide and deduced amino-acid sequences was tentatively given a number, as in a previous study (Takano et al. 2007). All known EHMfas1-specific units, CN3, CN5, CN7, and CN3'C2, were also observed in P19-061405; however, the combination pattern of the repeating unit was different. Although P19-061405 was not classified into any known genotype, based on the nucleotide sequence, it was classified into genotype D based on the deduced amino-acid sequence in the polymorphic region.

Many SREHP genes of *E. histolytica* have been sequenced for genotyping (Li et al. 1992; Clark and Diamond 1993; Kohler and Tannich 1993; Stanley et al. 1990; Ayeh-Kumi et al. 2001; Haghighi et al. 2002, 2003). The reported SREHP gene sequences of EHMfas1, P19-061405 and *E. histolytica* KU27 (genotype I), were compared (Fig. 3). Each unit of the nucleotide and deduced amino-acid sequences was tentatively given a number, as in a previous study (Takano et al. 2007). All known EHMfas1-specific units, SN2, SN5, SN9, SN17, SN20, and SN3'C2, were also observed in P19-061405, but the combination pattern was different. The SN16 and DEE insertion, i.e., the second EHMfas1-specific insertion, were not observed in P19-061405. The nucleotide and deduced amino-acid sequences of P19-061405 were not classified into any of the known genotypes.

Locus 1–2 (also known as a non-coding short tandem repeat, D-A; Ali et al. 2005) of EHMfas1 and P19-061405 was directly sequenced and compared with the reported genotypes of *E. histolytica* (Zaki and Clark 2001; Haghighi et al. 2002, 2003). A number was tentatively assigned to each unit of the nucleotide sequences (Fig. 4). The nucleotide sequences of locus 1–2 were constructed from combinations of the 5'-conserved region, an 8 bp-repeating polymorphic region (8L1, 8L2, 8L3, and 8L4), intra-conserved region 1 (CL1, CL2, CL3, CL4, CL5,

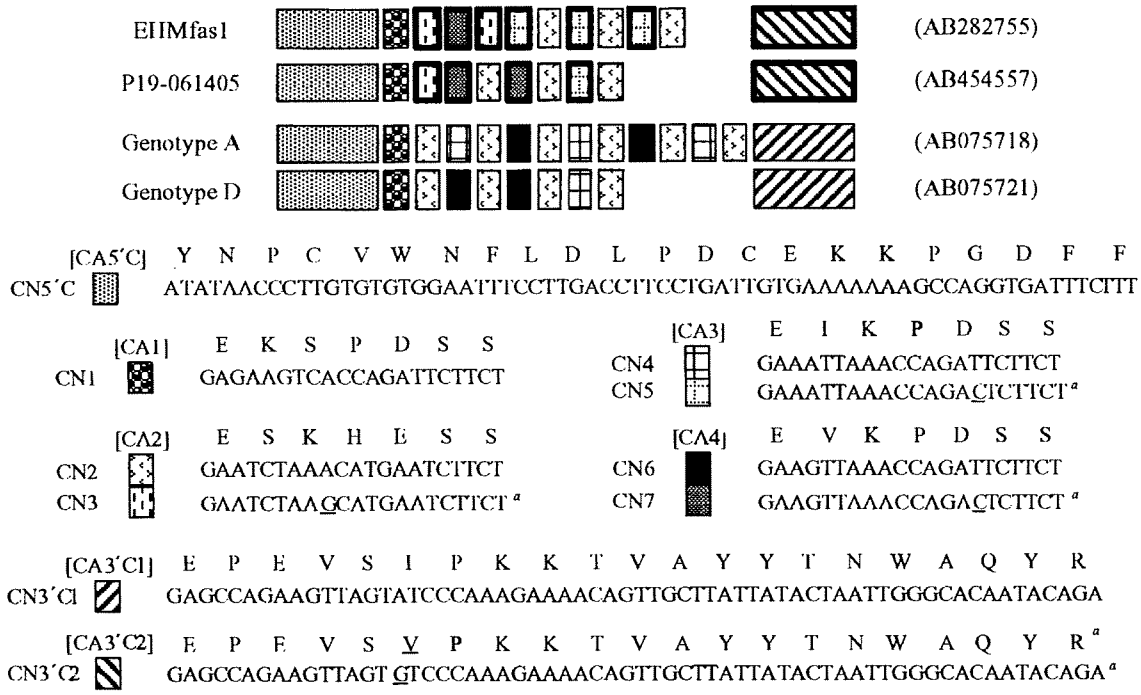

Fig. 2 Schematic representation of polymorphism in the repeat-containing region of the chitinase gene among simian *E. histolytica*-like strains and genotype A and D of *E. histolytica*. Nucleotide sequences pattern was shown. Each of nucleotide and deduced amino-acid sequences of unit was tentatively given a number. Nucleotide and deduced amino-acid sequences of these units are also shown. *Enclosed units with bold line* were simian *E. histolytica*-like strain-specific units. Simian *E. histolytica*-like strain-specific mutations in nucleotide and deduced amino-acid sequences are *underlined*. *a* Simian *E. histolytica*-like strain-specific unit sequences

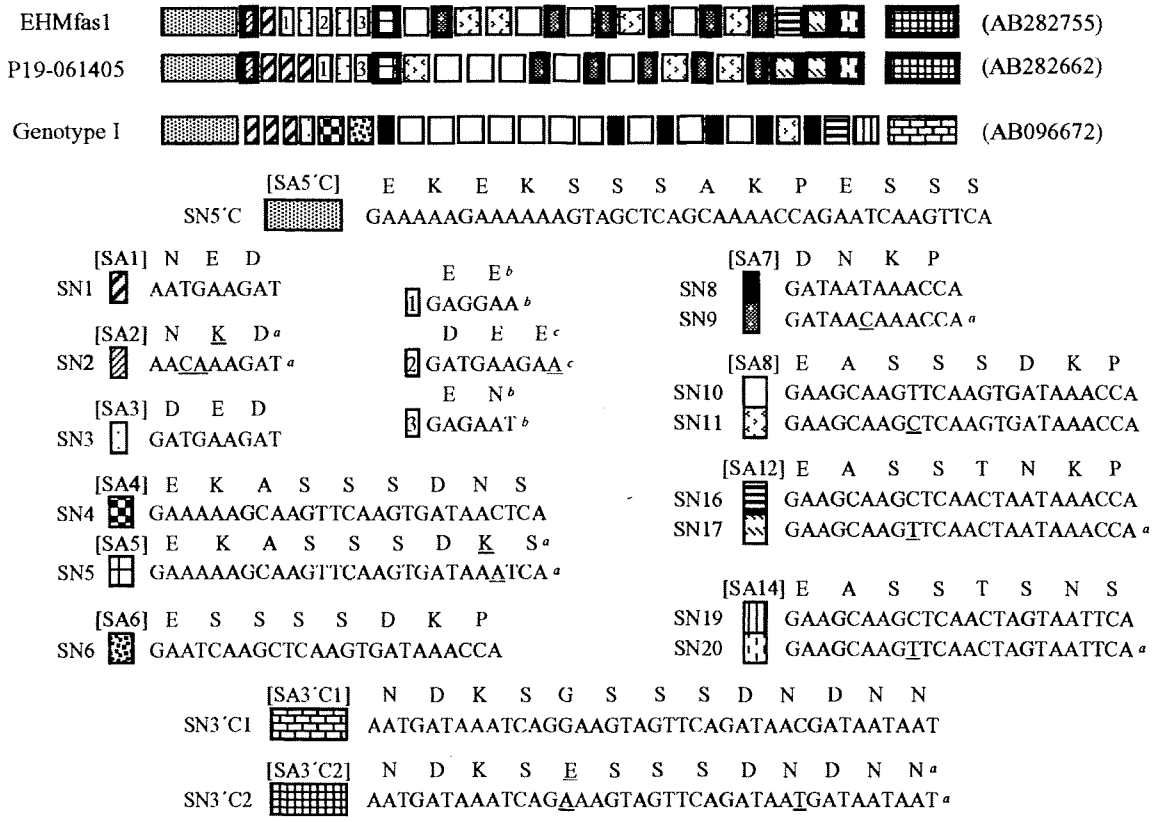

Fig. 3 Schematic representation of polymorphism in the repeat-containing region of the SREHP gene among simian *E. histolytica*-like strains and genotype I of *E. histolytica*. Nucleotide sequences pattern was shown. Each nucleotide and deduced amino-acid sequence of unit was tentatively given a number. Nucleotide and deduced amino-acid sequences of these units are also shown. *Enclosed units with bold line* were simian *E. histolytica*-like strain-specific units. Simian *E. histolytica*-like strain-specific mutations in nucleotide and deduced amino-acid sequences are *underlined*. *a* Simian *E. histolytica*-like strain-specific unit sequences. *b* Simian *E. histolytica*-like strain-specific block insertions. *c* EHMfas1-specific block insertion

CL6, and CL7), a 9-bp-repeating polymorphic region (9L1, 9L2, 9L3, 9L4, 9L5, and 9L6), intra-conserved region 2 (CL6, CL9, CL10, and CL11), a 12-bp-repeating polymorphic region (12L1, 12L2, 12L3, and 12L4), and the 3′-conserved region. The 8L1, 8L3, CL1, CL5, CL6, 9L1, 9L2, 9L4, and 12L3 units were common to simian *E. histolytica*-like strains and *E. histolytica*. On the other hand, 8L4, CL2, CL4, 9L3, 9L5, CL11, 12L2, and 12L4, were simian *E. histolytica*-like strain-specific mutated units. These mutated units corresponded to the 8L3, CL1, CL3, 9L2, 9L4, CL10, 12L1, and 12L3 units, with a single-nucleotide substitution in each unit, respectively. The CL8 was also a simian *E. histolytica*-like strain-specific unit that corresponded to CL7 with a four-nucleotide deletion (CCCT). Most units observed in *E. histolytica* were also observed in simian *E. histolytica*-like strains; however, all 12L1 were changed to 12L2 in the simian *E. histolytica*-like strains, and the CL9 was missing in the simian *E. histolytica*-like strains. Furthermore, 8L2 was observed only in EHMfas1 and corresponded to 8L1 with a double-nucleotide substitution.

Discussion

In this study, genetic similarities between EHMfas1 and P19-061405 and differences between simian *E. histolytica*-like strains and *E. histolytica* were revealed. EHMfas1 was also a virulent strain as P19-061405. The similar zymodeme patterns of EHMfas1 and P19-061405 have not been classified into any known patterns (Takano et al. 2007; Tachibana et al. 2007). Although some deduced amino acids were changed, the genetic similarities of HXK, GPI, and PGM supported the results of the isoenzyme analyses. HXK, GPI, and PGM of the simian *E. histolytica*-like strains were obviously more similar to *E. histolytica* than *E. dispar*. It is considered that EHMfas1 and P19-061405 are the same species, despite the fact that these strains were isolated from different host monkey species and a different habitat. Thus, simian *E. histolytica*-like amebas likely naturally infect macaques as a counterpart to *E. histolytica* in human.

Phylogenetic studies also indicated that EHMfas1 and P19-061405 are the same species and are closely related to *E. histolytica*. Nucleotide sequences of the 18S rDNA